Response to editor:

We have carefully gone through all the comments and suggestions raised by the two reviewers. To address these issues, we have included additional information and calculation results. The structure of the manuscript was also rearranged to improve the readability and logical structure. Please find the point-by-point response to the reviewers and the marked revised manuscript below:

Response to reviewer #1

General comments

The article “NH_3-promoted hydrolysis of NO_2 induces explosive growth in HONO” discussed the mechanism behind explosive HONO formation during field observation in a rural site in North China. In general, the phenomenon, confidence of related evidence were sufficient to show the role of NH_3 in HONO productions via heterogeneous reaction during fog/smoke events. The observation data was well linked to possible atmosphere processes, which might greatly promote the understanding of HONO sources and thus providing new insights of pollution control strategies for China. Yet, the authors should address several minor points to make the narrative as well as the deduction more convincible.

Minor suggestions

1. First, it is well known that the HONO is extremely reactive especially during daytime. For most of the cases, the author noted that the rarely seen Ozone was the evidence that there was no sufficient sunlight. It seems that the Ozone concentration was used as an indicator of UV radiation and possible photochemistry reactions (line213-line218). But the Ozone could be titrated by NO, which was often measured a high level during nighttime in North China. Therefore, even the Ozone

was observed to be nearly zero, there might be enough UV radiation for the quick HONO photolysis. This leads to a further question - can we trust the HONO measurements by a denuder system? The annular denuder method of detecting might have artefacts regarding to measuring HONO due to: 1. Hydrolysis of NO2 onto wet surface; 2.Aqueous reaction of S(IV) with NO2 in the solution(Spindler, Hesper et al. 2003, Nie, Ding et al. 2015). The second reaction could likely be accelerated in the presence of ammonia as reported in the previous studies (Cheng, Zheng et al. 2016, Wang, Zhang et al. 2016). Therefore, it is strongly recommended that the authors should conducted some validation of the HONO data from IGAC, given the fact that the HONO data obtained by denuder system need further calculation/reprocessing.

Response:

Thank you for your valuable comments. During the campaign in 2016, the IGAC instrument was borrowed from the Fortelice International Company. Unfortunately, circumstances do not allow us to borrow the instrument again for additional experiments, but we hope to prove the instrument reliable using the entire measurement dataset.

As already pointed out in your comment, instruments using wet denuders to collect gaseous HONO can cause sampling artefacts mainly via two pathways: 1) the NO_2 conversion on the surface of the sampling tube and the wet denuder and 2) the reaction of NO_2 with S(IV) in the absorption solution in wet denuder (Nie et al., 2015). The second pathway is avoided in IGAC by using a dilute ($5x10^{-3}$ M) H_2O_2 solution, which quickly converts S(IV) to S(VI). The first artefact is often corrected for using a linear correction using slopes of 0.83-0.85. (Su, 2008;Qiang et al., 2014;Nie et al., 2015). Qiang et al. (2014) compared HONO measurements by an instrument called GAC-IC with that of LOPAP and found generally good agreement between both instruments after using a linear correction. Note that such linear adjustments do not alter the overall variation characteristics of HONO. The GAC and MARGA systems all consist of horizontally positioned wet denuders, in which the absorption solution might accumulate and cause additional artifacts. The IGAC system uses a vertically installed wet denuder, guaranteeing for the smooth outflow of the absorption solution. Overall, it is reasonable to believe that IGAC is able to capture the variation characteristics of HONO, even if a slope of 0.83 were used to correct the HONO data, the peaks would still reach 8.8, 7.9, 9.5 and 14.6 ppb, which is still very high.

Further, to prove that the observed peaks were not caused by instrument sampling artefacts, we analyzed the variation of observed HONO with SO_2, NO_2 and NH_3 during 15th Oct. to 25th Nov. 2016 (Fig.1). High HONO concentrations were typically observed under low SO_2 conditions, which proves that the sampling artefact due to the reaction of S(IV) and NO_2 in the wet denuder could be neglected. If the instrument would cause sampling artefacts due to NO_2 conversions, the high HONO concentrations should have been frequently observed under high NO_2 concentrations, which was not the case. The NO_2 concentrations at the occurrence time of the 4 peaks were all below 50 ppb. NO_2 often exceeded 50 ppb during the campaign, however, HONO stayed below 7 ppb throughout the whole campaign, except for the 4 cases studied in this work.

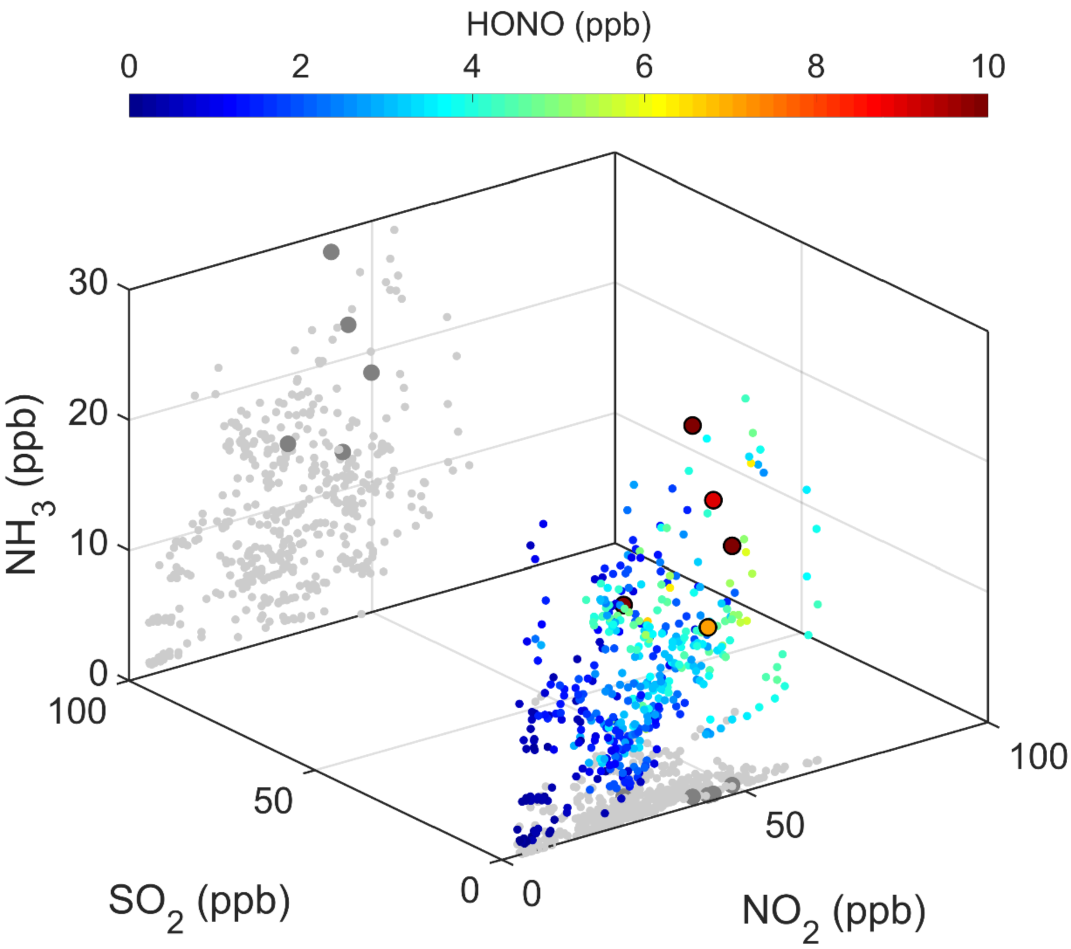

Figure 1 Variation of HONO with SO_2 (y-axis), NO_2 (x-axis) and NH_3 (z-axis) during 15th Oct. to 25th Nov. 2016, with the large dots indicating the data points with HONO exceeding 7 ppb

2. The second point will be lying in the mechanism discussions. Though R1 could not explain the increasing nitrate (line 260-261), but attributing all the SIA (secondary inorganic aerosols) increase due to HONO formation and thus denying the role of R1 seems to be assertive. Actually, the nitrite in the aqueous phase might have produced OH radicals in aerosol liquid water or fog droplets (Vione, Maurino et al. 2006). It would be good to illustrate or maybe quantify the relative contribution of R1 v.s. R2 to HONO production as well as SIA production.

Response:

We thank the reviewer for these valuable comments and suggestions, which has greatly helped us in improving our manuscript. We took the advice in this comment and estimated the relative contributions of R1 and R2 to HONO production using the following assumptions.

First, we assume the observed increase in sulfate (d[SVI]/dt) was caused by the reaction of SO_2 with H_2O_2, O_3, NO_2, TMI (Fe^{3+} and Mn^{2+}). Calculations were performed according to Cheng et al. (2016a), using the same pH dependent TMI concentrations and the actual SO_2, H_2O_2, O_3 and NO_2 concentrations in our measurements (Table 1). For the two fog episodes on 4th and 5th Nov. 2016, the mean diameter of fog droplets was assumed to be 7.0 μm and the liquid water content was assumed to be 0.3 g m^{-3} according to Shen et al. (2018). For the haze episodes on the 11th and 14th Nov. 2016, the mean aerosol diameter under ambient conditions was estimated to be 0.65-1.22 and 0.9 μm, while the liquid water content was calculated to decrease from 3.4×10^{-4} to 7.8×10^{-5} on the 11th Nov and assumed to be 0.01 g m^{-3} on the 14th Nov. during the transition from fog to haze. The sulfate production rate and relative contribution of the each oxidation pathway to the total sulfate production rate was obtained and depicted in Figure 2. For the two fog episodes, assuming pH=6, the estimated average sulfate production rates are 11.7 and 31.6 approximately 4 times of that observed within PM2.5, which is clearly an underestimation, considering the liquid water content of fog droplets are at least a magnitude higher than that of aerosols. For the two haze episodes, using the pH values estimated using ISORROPIA (forward mode and metastable assumption (Song et al., 2018)), the estimated average sulfate production rates are 0.06 and 1.8, about 10% of that observed within PM2.5. Following the calculations of Cheng et al. (2016a), we have considered the influence of ionic strength on the reaction rates and set constraints on the maximum ionic strength (I_{max}), which might have caused underestimations for all reaction routes, since the calculated ionic strength commonly exceeded I_{max}. Underestimated transition metal ion concentrations may also be partly responsible for the underpredicted sulfate production, since the TMI catalysis route has recently be pointed out to be the dominant SO_2 heterogeneous oxidation pathway (Shao et al., 2019). Additionally, there also might be other neglected SO_2 oxidation pathways, which will lead to overestimates in the sulfate fraction produced by the NO_2 oxidation pathway.:

$$\frac{d[HONO]}{dt}_{R1} = 2 \times frac_{SO_2+NO_2} \times \frac{d[SVI]}{dt}_{obs}. \tag{1}$$

where $frac_{SO_2+NO_2}$ is the contribution fraction of the NO_2 oxidation pathway to the total sulfate production. Note that the calculated HONO production rate can only represent the production within $PM_{2.5}$.

Table 1. The trace gas concentrations, liquid water content, mean diameter and temperature used to calculate the heterogeneous sulfate production

Date	Time (LT)	SO_2 (ppb)	H_2O_2 (ppb)	NO_2 (ppb)	O_3 (ppb)	LWC (g m^{-3})	D_p (µm)	T (K)
4th Nov	9:00	0.18	0.26	45.3	1.53	0.3	7.00	277.8
	10:00	0.17	0.29	48.8	1.56	0.3	7.00	278.4
	11:00	0.28	0.34	49.9	1.78	0.3	7.00	278.7
5th Nov.	10:00	0.16	0.19	44.6	2.90	0.3	7.00	278.8
	11:00	0.39	0.21	44.0	3.39	0.3	7.00	279.6
	12:00	1.19	0.30	45.1	5.72	0.3	7.00	281.3
11th Nov.	7:00	0.40	0.52	30.7	1.41	3.4 e^{-4}	1.22	271.2
	8:00	0.44	0.71	33.0	1.53	2.1e^{-4}	0.73	272.3
	9:00	1.61	0.89	32.7	1.83	7.8e^{-5}	0.65	274.8
14th Nov.	11:00	1.27	0.32	41.6	1.52	0.01	0.90	278.1

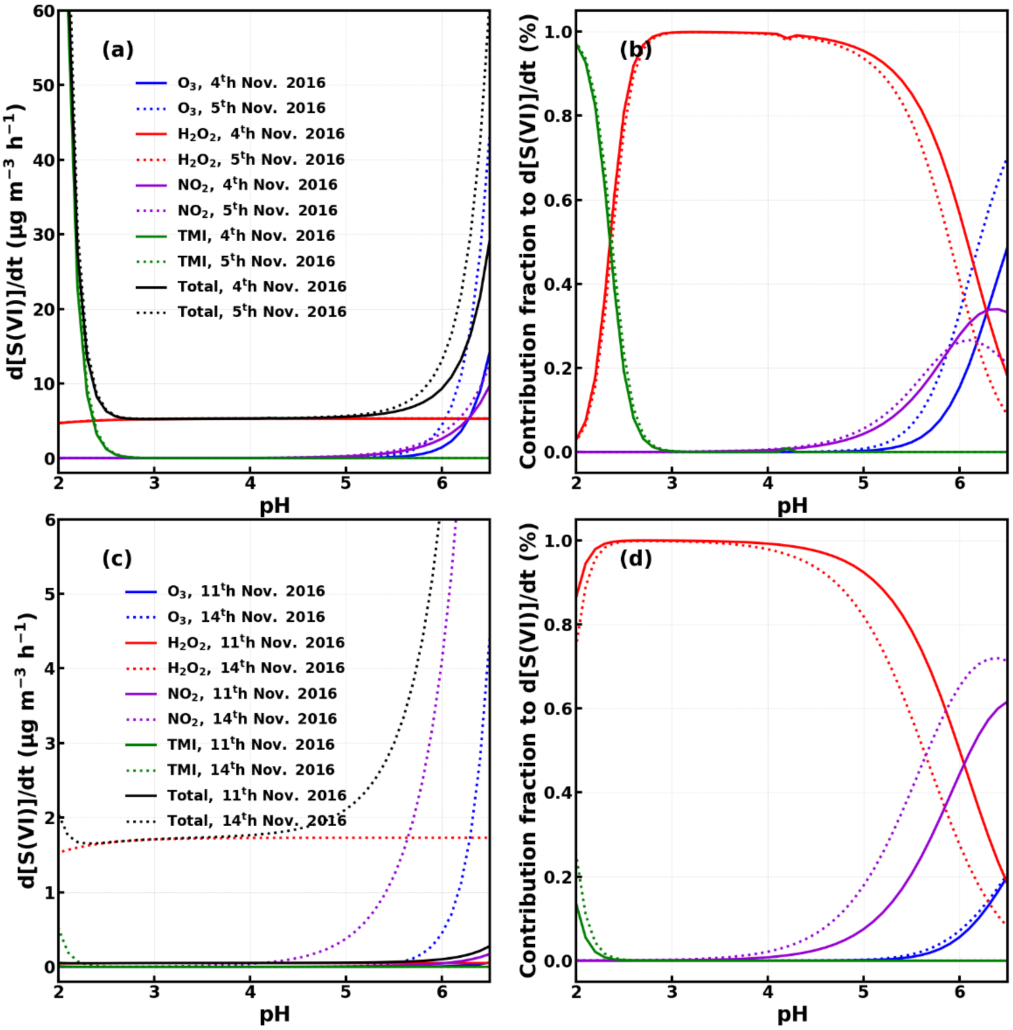

Figure 2. Calculated average sulfate production (a,c) and contribution fraction b,d) from SO_2 oxidation by H_2O_2, NO_2, O_3, TMI under different pH values using methods described in (Cheng et al., 2016a) for the case episodes on 4th, 5th, 11th and 14th Nov. 2016.

Then, we further assume the observed nitrate production ($d[NO_3^-]/dt$) was caused by reaction R2 and by the reaction of NO_2 with OH radicals (k_{NO_2+OH}=3.2×10^{-12} cm^3 s^{-1}), the HONO production rate of R2 would be:

$$\frac{d[HONO]}{dt}_{R2} = \frac{d[NO_3^-]}{dt}_{obs} - k_{NO_2+OH}[NO_2][OH]. \tag{2}$$

The contribution fraction of the two reactions to the heterogeneous HONO production in aerosol and fog liquid water content can be calculated by:

$$f_{R1} = \frac{d[HONO]}{dt}_{R1} \Big/ \frac{d[HONO]}{dt}_{R1+R2} \quad \text{and} \quad f_{R2} = \frac{d[HONO]}{dt}_{R2} \Big/ \frac{d[HONO]}{dt}_{R1+R2}.$$

Assuming the pH of fog droplets falls within the range of 4 to 6, f_{R2} was estimated to range from range from 75.5 to 99.5% and from 81.2 to 99.5% during the 4th and 5th Nov. 2016, respectively. For the two haze events on 11th and 14th Nov., the f_{R2} corresponding to the pH values modelled by ISORROPIA would be 98.2% and 97.3%.

These results suggest that, reaction R2 is the dominant contributor to the heterogeneous HONO production, while R1 is more important under high pH conditions. Under the assumed upper limit of pH, R1 can contribute up to 24.5%, 18.8% to the observed HONO growth during the fog events. This is in accordance with results from Wang et al. (2016) and Cheng et al. (2016b), which suggested that R1 was more likely to happen during fog episodes or under NH_3 neutralized conditions (3,4). For the two haze events, R1 contributed very little (1.8% and 2.7%) to the observed HONO growth.

In summary, reaction R2 was the dominant contributor to the heterogeneous HONO production, while R1 only played a minor role during fog events and a negligible role during haze events. The above discussions were added to Sect. 4.2 in the revised manuscript.

Technical notes

1. Line 110-111: “Under highly polluted conditions such as our site”. Might have wrong grammar used.

Response:

Thank you for noticing, this sentence was rephrased as:

“Considering the severe pollution state the NCP is under, these measurement uncertainties are fully acceptable.”

2. Figure 3. The time label on X axis causes misunderstanding, might change to Date-Time format.

Response:

Thank you for the suggestion, to avoid confusion the x axis labels were changed to hours and the date was marked on top of the figure (see Fig.4 below in Response #3).

3. Figure 4. The unit of aerosol composition (nitrate/sulfate/ammonium) should be in mass concentration.

Response:

Thank you for the suggestion, the unit of aerosol composition was changed to µg m^{-3} in Figs. 2-4 (Figs. 3-5 below) and in the corresponding texts.

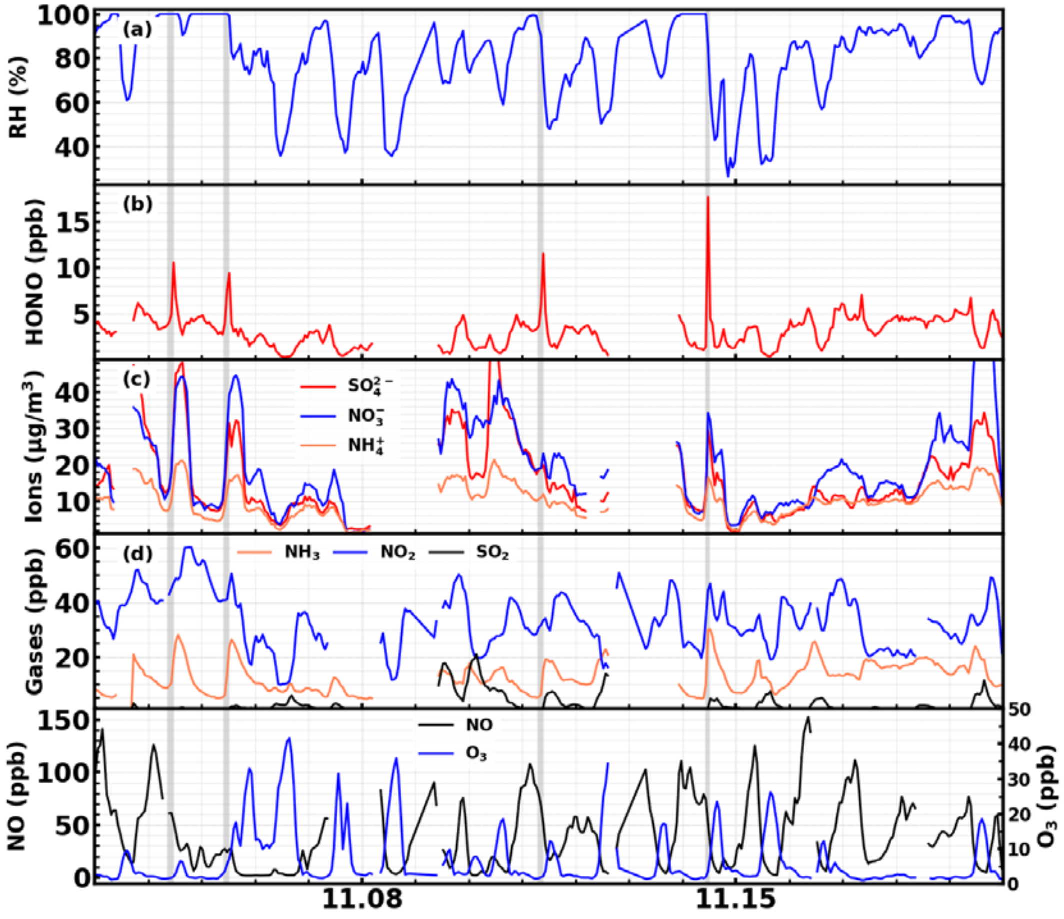

Figure 3. Time series of ambient **a)** RH; **b)** HONO; **c)** sulfate, nitrate, ammonium; **d)** NH_3, NO_3 and SO_2 during the observation period.

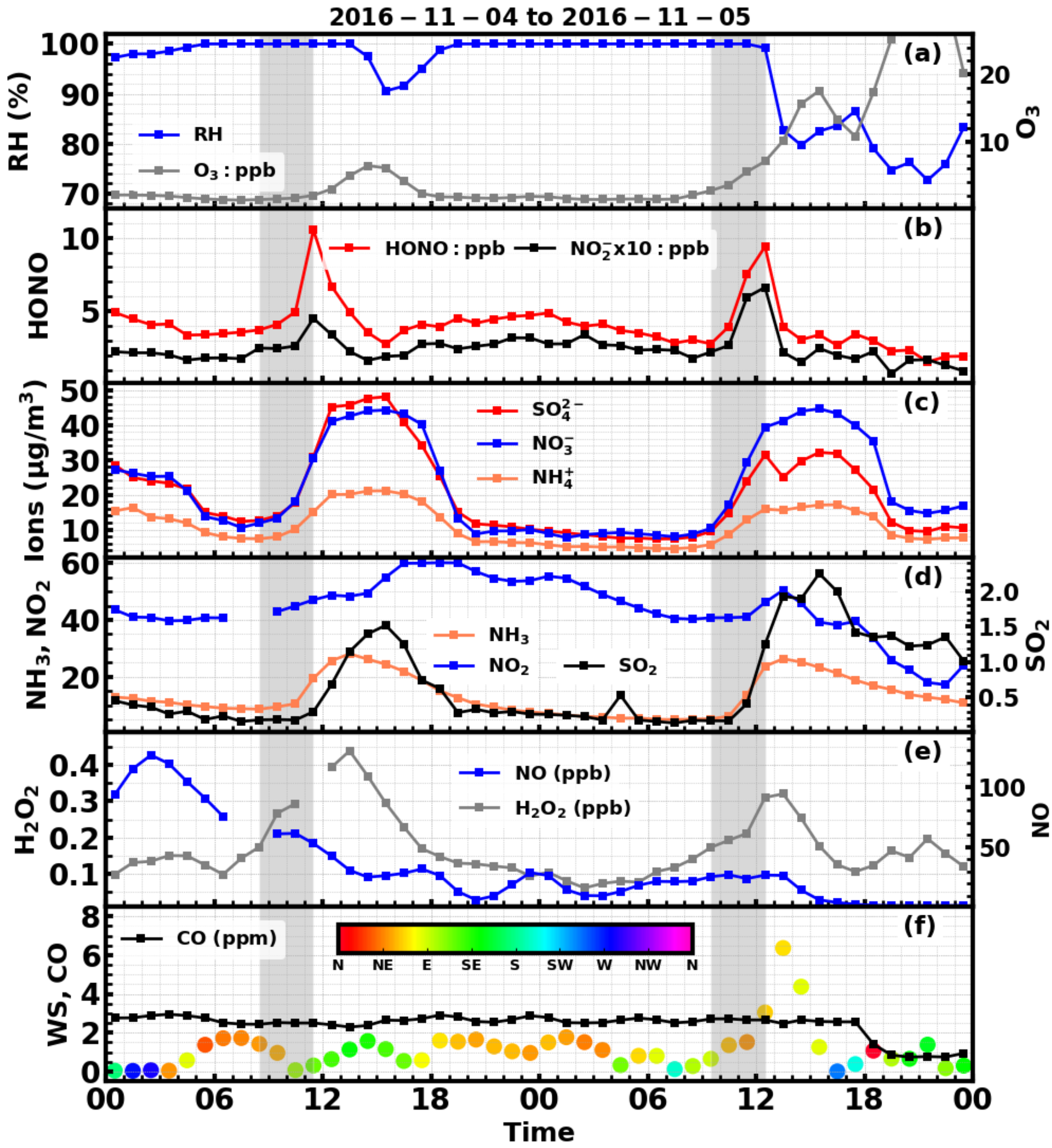

Figure 4 Time series of ambient **a)** RH,O_3, **b)**HONO, NO_2^-, **c)** SO_4^{2-}, NO_3^-, NH_4^+, **d)** NH_3, NO_2, SO_2, **e)** NO, H_2O_2, **f)** CO, wind speed and wind direction (colors of scatter points) from 11-04 to 11-05. Gray shaded areas represent periods of rapid increase of HONO.

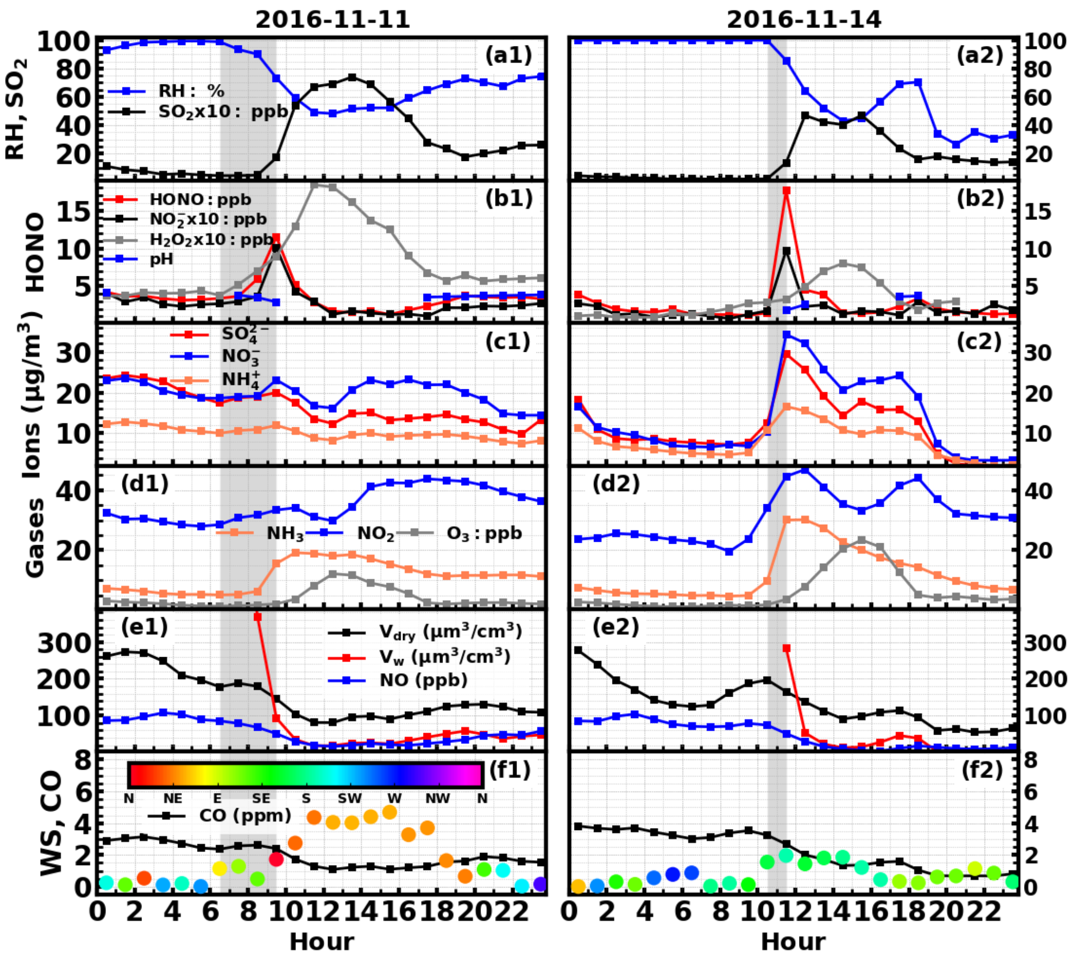

Figure 5 Time series of ambient **a)** RH, SO$_2$, **b)** HONO, NO$_2^-$, H$_2$O$_2$, aerosol pH, **c)** SO$_4^{2-}$, NO$_3^-$, NH$_4^+$,**d)** NH$_3$, NO$_2$, O$_3$, **e)** NO, volume concentrations of PM$_{2.5}$ in dry state (V$_{dry}$), volume concentrations of liquid water (V$_w$), **f)** CO, wind speed and wind direction during **1)** 11th Nov. 2016 and **2)** 14th Nov. 2016. Gray shaded areas represents periods of rapid increase of HONO.

Reference

Cheng, Y., Zheng, G., Wei, C., Mu, Q., Zheng, B., Wang, Z., Gao, M., Zhang, Q., He, K., Carmichael, G., Pöschl, U., and Su, H.: Reactive nitrogen chemistry in aerosol water as a source of sulfate during haze events in China, Science Advances, 2, e1601530, 10.1126/sciadv.1601530, 2016a.

Cheng, Y., Zheng, G., Wei, C., Mu, Q., Zheng, B., Wang, Z., Gao, M., Zhang, Q., He, K., Carmichael, G., Pöschl, U., and Su, H.: Reactive nitrogen chemistry in aerosol water as a source of sulfate during haze events in China, Science Advances, 2, 10.1126/sciadv.1601530, 2016b.

Nie, W., Ding, A. J., Xie, Y. N., Xu, Z., Mao, H., Kerminen, V. M., Zheng, L. F., Qi, X. M., Huang, X., Yang, X. Q., Sun, J. N., Herrmann, E., Petäjä, T., Kulmala, M., and Fu, C. B.: Influence of biomass burning plumes on HONO chemistry in eastern China, Atmos. Chem. Phys., 15, 1147-1159, 10.5194/acp-15-1147-2015, 2015.

Qiang, Y., Hang, S., Xin, L., YaFang, C., KeDing, L., Peng, C., JianWei, G., Song, G., Min, H., LiMin, Z., Tong, Z., and YuanHang, Z.: Daytime HONO formation in the suburban area of the megacity Beijing, China, Science China(Chemistry), 57, 1032-1042, 2014.

Shao, J., Chen, Q., Wang, Y., Lu, X., He, P., Sun, Y., Shah, V., Martin, R. V., Philip, S., Song, S., Zhao, Y., Xie, Z., Zhang, L., and Alexander, B.: Heterogeneous sulfate aerosol formation mechanisms during wintertime Chinese haze events: Air quality model assessment using observations of sulfate oxygen isotopes in Beijing, Atmos. Chem. Phys. Discuss., 2019, 1-28, 10.5194/acp-2018-1352, 2019.

Shen, C., Zhao, C., Ma, N., Tao, J., Zhao, G., Yu, Y., and Kuang, Y.: Method to Estimate Water Vapor Supersaturation in the Ambient Activation Process Using Aerosol and Droplet Measurement Data, Journal of Geophysical Research: Atmospheres, 123, 10606-10619, doi:10.1029/2018JD028315, 2018.

Su, H.: HONO: a study to its sources and impacts from field measurements at the sub-urban areas of PRD region, Peking University, Beijing, China, 2008.

Wang, G., Zhang, R., Gomez, M. E., Yang, L., Levy Zamora, M., Hu, M., Lin, Y., Peng, J., Guo, S., Meng, J., Li, J., Cheng, C., Hu, T., Ren, Y., Wang, Y., Gao, J., Cao, J., An, Z., Zhou, W., Li, G., Wang, J., Tian, P., Marrero-Ortiz, W., Secrest, J., Du, Z., Zheng, J., Shang, D., Zeng, L., Shao, M., Wang, W., Huang, Y., Wang, Y., Zhu, Y., Li, Y., Hu, J., Pan, B., Cai, L., Cheng, Y., Ji, Y., Zhang, F., Rosenfeld, D., Liss, P. S., Duce, R. A., Kolb, C. E., and Molina, M. J.: Persistent sulfate formation from London Fog to Chinese haze, Proceedings of the National Academy of Sciences, 113, 13630, 2016.

Response to reviewer #2

General comments

The paper “NH_3-promoted hydrolysis of NO_2 induces explosive growth in HONO” by Wanyun Xu et al is joining the long series of scientific work aiming at elucidating the HONO sources that have been published these past twenty years. Considering the major role of HONO in the initiation of the photo-oxidation cycles in the troposphere, any significant work related to the processes that give birth to this key molecule are necessarily important (Kleffmann et al, 2007). Wanyun Xu et al are mostly founding the exploitation of their results on a methodology based on recent papers only and are often disregarding the precious findings of the early times. Nevertheless, they provide here an attempt to exploits a limited set of data obtained in heavily polluted environment that is not without any merit. Overall, I have many minor points to discuss but, for me, one major point is shining a doubtful light over the whole study: it concerns the reliability of the HONO/NO_2- measurements themselves. The reliable measurement of HONO at low level in the atmosphere has been an analytical challenge for decades. Many groups have worked on various analytical concepts ranging from long path spectroscopy, optical cavities, ionic chromatography or dye formation combined with absorption within waveguide tubing or HPLC analysis.

Because of HONO high reactivity the risk of underestimation of its concentration is often high. In the same time, because of the multiplicity of its heterogeneous sources the risk of positive artefact and unwanted HONO generation in/nearby the system is high too. This is why, even when the measurement principle itself was mature, the sampling condition was often found to be a key parameter for trustable measurements, which has led to important work on the design of inlets, minimizing surfaces, choosing material.

Each of these instrumental concept has required extensive characterization works and a few inter-comparison exercises have demonstrated how large the discrepancies can be (Keuken et al, 1990; Stutz et al, 2009; Kleffmann et al, 2006; Pinto et al, 2014).

Major issues

1. In the present paper, the whole experimental strategy relies on the performance of the so-called In situ Gas and Aerosol Compositions Monitor (IGAC, Fortelice International Co.,Taiwan) as both HONO/NO_2- and NH_3 concentrations – the two key species of the present study - are monitored using this instrument. The available information about this device are scarce: IGAC consists in a combination of a wet annular denuder and a particle into liquid sampler. Unfortunately it has been poorly characterized in general and none of the reference provided in the paper are relevant for HONO measurements. In particular, while citing Liu et al, 2017a to claim “the instrument has shown good performance in the past” or quoting Young et al, 2016, one can only regret that nothing in these papers really concern nitrous acid or nitrite ions measurements. Further, Young et al, 2016 indicate that the performance of IGAC were poor concerning the measurement of ammonia.

   On my side, considering the IGAC experimental device and condition of use, I especially worry about the use of “a dilute H_2O_2 solution to collect the gases”. If one refer to Young et al, 2016 the “dilute solution” is a $5x10^{-3}$ M solution (why not mentioning the concentration in the experimental section?) which is used to “assure the oxidation of SO_2 to SO_4^- and prevents microbial growth “. For me, it is highly probable that such a concentration of such a strong oxidation agent could induced artefacts in the HONO measurement: - in the absence of precursors, it may induce a negative artefact by oxidizing nitrites to nitrates but, on the contrary - in the presence of enough reduced nitrogenous species (such as ammonia) it may forms HONO. In this case this would both affect NH_3 and HONO measurements and would probably lead to a correlation between both species (if ammonia is in excess). Considering the poor level of details provided in the experimental section, the lack characterization experiments demonstrating the ability of IGAC to measure HONO (especially in the presence of ammonia) and the strong suspicion of artefacts exactly relevant from the main paper conclusion, I strongly recommend to provide the experimental evidences that demonstrate the suitability of the measurement protocol for both NH_3 and HONO before considering any publication.

Response:

During the campaign in 2016, the IGAC instrument was borrowed from the Fortelice International Company. Unfortunately, circumstances do not allow us to borrow the instrument again for additional experiments, but we believe the entire dataset itself may be able to prove itself reliable.

1) **On the concern that the IGAC instrument showed "poor" performance in respect of ammonia measurements**, we would thank the reviewer for the careful inspection of our work and for raising this concern, which indeed needs to be addressed to solidify our work.

   To evaluate the NH_3 data quality measured by IGAC, we compared them against NH_3 measurements of an LGR economical ammonia analyzer (DLT-100, Los Gatos Research, USA). Note that the IGAC instrument, the SMPS+APS system, the humidified nephelometer system and the AL2021 H_2O_2 analyzer were housed in an air-conditioned container located on the northern edge of the Gucheng site, while the trace gas instruments (including SO_2, NO_x, CO and NH_3) that carried out long-term measurements were housed on the second floor of a two story building located on the southern edge of the Gucheng site. Details on the LGR NH_3 measurements can be found in Meng et al. (2018).

   In Young et al. (2016), IGAC showed marginally acceptable performance test result for NH_3, with the intercept of the linear fitting meeting the evaluation criteria, while the slope of 0.59 did not. They pointed out that the underestimation in IGAC NH_3 measurements was probably caused by losses on the sampling tube wall. This indicates that the NH_3 measured by IGAC are systematically lower, which high possibly has no great influence on the relative variation pattern of NH_3, which we are concerned of in this study. It should be noted that Young et al. (2016) performed

NH_3 measurements and validation in the concentration range of 0 to 16 ppb. Liu et al. (2017) performed NH_3 measurements with IGAC in urban Beijing, with NH_3 varying between 0 to 35 ppb, which is closer to the observed NH_3 range in our campaign. The measurements were validated against ISORROPIA II simulations and reached good agreement (R^2>0.9). Teng et al. (2017) observed that LGR measurements were far larger than those measured based on wet denuders (with a slope near 0.7) and suggested the overestimation of LGR was possibly caused by interference of water vapor. Overall, we believe that even though the IGAC system may not be as precise as other specific NH_3 analyzers, if it can capture the variation characteristics of NH_3, it would be enough to prove the proposed the HONO production pathway.

Overall, the comparison of the NH_3 measured with LGR against that of IGAC showed a slope of 0.91 (R=0.63) and an intercept of 6.86 (Fig.1a). If data measured under high RH conditions (RH≥80) were excluded, an obvious improvement in the comparison results would be achieved (Fig.1b), with a slope of 1.03 (R=0.74) and an intercept of 2.89. This indicates that, high discrepancies between the two instruments mostly occur at high relative humidity, where LGR measurements are significantly higher than those of IGAC. Since these discrepancies were linked to high RH conditions, it is more likely that they were caused by the LGR instrument that overestimates NH_3 due to absorption interference of water vapor. The variation of NH_3 measured by LGR and IGAC during the four episode cases is shown in Fig. 2. Although LGR showed higher NH_3 concentrations (especially during nighttime when fog prevailed and RH was near 100), the variation characteristics were the same between the two instruments, all displaying rapid increases during the explosive HONO formation events. Thus, we believe it is appropriate to use the IGAC measured NH_3 for our discussions.

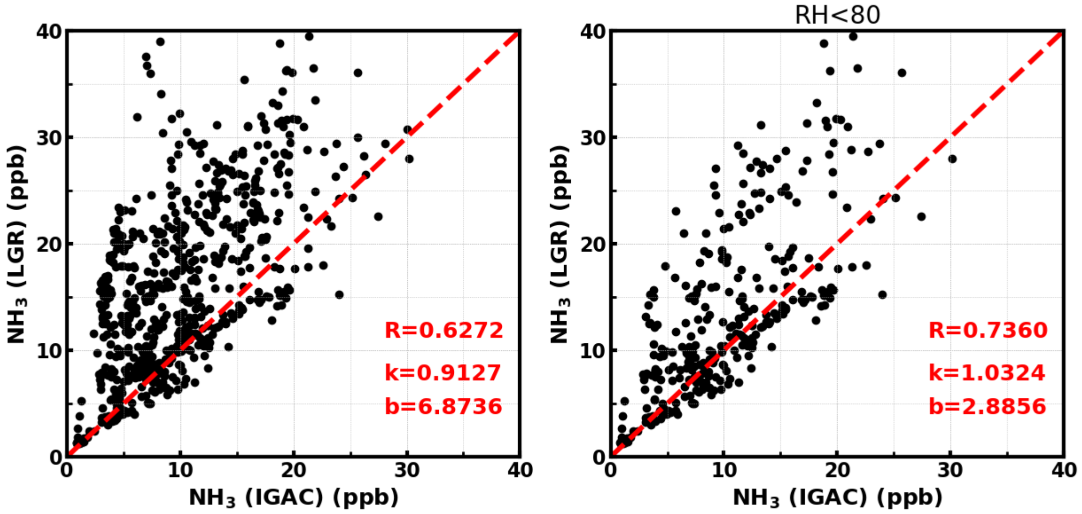

Figure 1 Comparison between NH$_{3,IGAC}$ and NH$_{3,LGR}$ using a) all measurement data and b) data associated with RH<80.

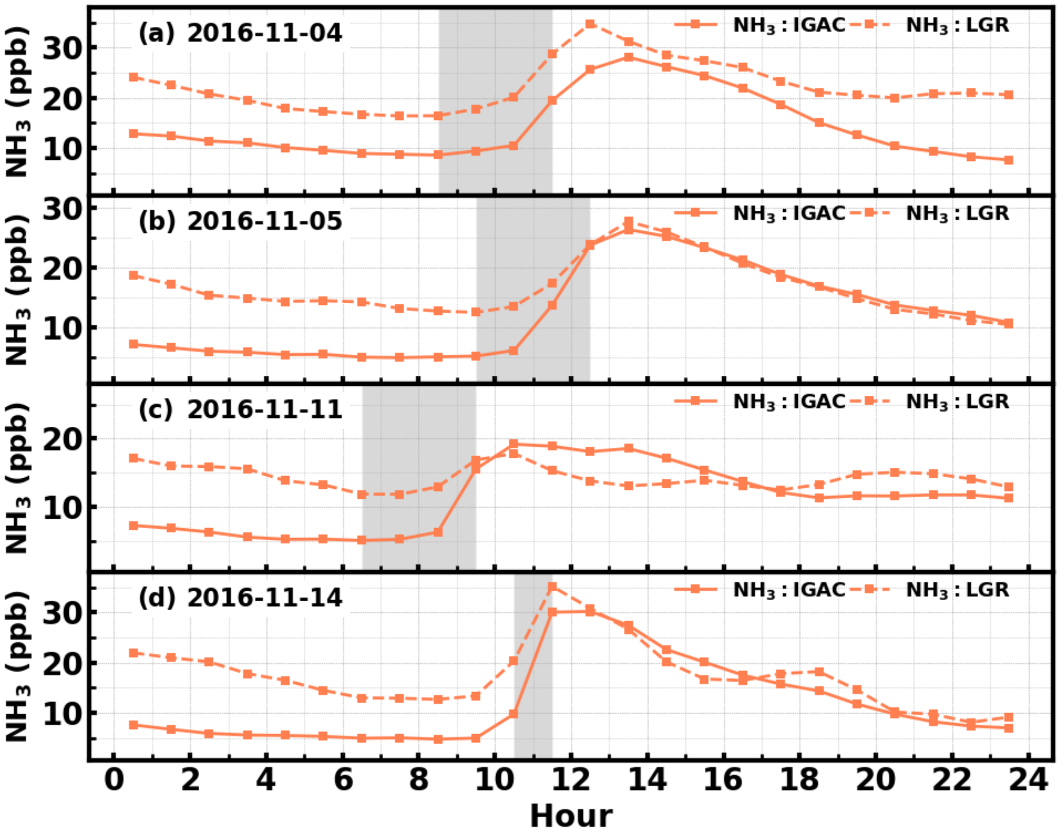

Figure 2 Time series of NH$_{3,IGAC}$ (solid) and NH$_{3,LGR}$ (dashed) during a) 4th Nov., b) 5th Nov., c) 11th Nov. 2016 and d) 14th Nov. 2016. Gray shaded areas represents periods of rapid increase of HONO.

We hope that this gives the reviewer and readers more confidence in the measurement results of IGAC concerning NH$_3$. In the revised manuscript, the following was added to Sect. 2 to provide the readers with more insight into the NH_3 measurements and data quality:

"A comparison between NH_3 observed by IGAC and by an economical NH_3 analyser (LGR, DLT-100, details see Meng et al. (2018)) yielded an overall slope of 0.91 with R=0.63 (Fig.S1a). A better comparison result (slope of 1.03, R=0.74) would be obtained if data associated with RH≥80 were excluded (Fig. S1b). The overestimation of LGR instruments compared to denuder based instruments has also been reported in Teng et al. (2017), suggesting possible interference of water vapor on NH_3 measurements. As can be seen in Fig S2., both instruments captured the same the diurnal variation of NH_3 during the four case episodes in this study, which proves that the IGAC instrument was able to capture the overall variation trends of NH_3. Since both instruments have their uncertainties, we decided to use the NH_3 measured by the IGAC instrument for better consistency with the other data."

2) **On the concern, whether the IGAC instrument can accurately measure HONO,** the performance of IGAC in terms of HONO measurements has indeed not been validated against measurements from other instruments at present. A recent work compared WRF-CHEM simulated HONO against measurements by IGAC and found good agreement between the two of them (Feng et al., 2018). The IGAC instrument is not as widely used as the MARGA system, which shares similar design and principles as IGAC and has been often used to measure HONO in the past (Xie et al., 2015;Nie et al., 2015). Similar measurement systems have been widely applied to study the variation of HONO (Su et al., 2008;Yang et al., 2017;Gu et al., 2009;Qiang et al., 2014). Instruments using wet denuders to collect gaseous HONO can cause sampling artefacts mainly via two pathways: 1) the NO_2 conversion on the surface of the sampling tube and the wet denuder and 2) the reaction of NO_2 with S(IV) in the absorption solution in wet denuder (Nie et al., 2015). The second pathway is avoided in IGAC by using the dilute ($5x10^{-3}$ M) H_2O_2 solution, which quickly converts S(IV) to S(VI). The first artefact is often corrected

for using a linear correction using slopes of 0.83-0.85. (Su, 2008;Qiang et al., 2014;Nie et al., 2015). Qiang et al. (2014) compared HONO measurements by an instrument called GAC-IC with that of LOPAP and found generally good agreement between both instruments after using a linear correction. Note that such linear adjustments do not alter the overall variation characteristics of HONO. The GAC and MARGA systems all consist of horizontally positioned wet denuders, in which the absorption solution might accumulate and cause additional artifacts. The IGAC system uses a vertically installed wet denuder, guaranteeing for the smooth outflow of the absorption solution. Overall, it is reasonable to believe that IGAC is able to capture the variation characteristics of HONO, even if a slope of 0.83 were used to correct the HONO data, the peaks would still reach 8.8, 7.9, 9.5 and 14.6 ppb, which is still very high.

To further prove that the observed peaks were not caused by instrument sampling artefacts, we analyzed the variation of observed HONO with SO_2, NO_2 and NH_3 during 15th Oct. to 25th Nov. 2016 (Fig.3). High HONO concentrations were typically observed under low SO_2 conditions, which proves that the sampling artefact due to the reaction of S(IV) and NO_2 in the wet denuder could be neglected. If the instrument would cause sampling artefacts due to NO_2 conversions, the high HONO concentrations should have been frequently observed under high NO_2 concentrations, which was not the case. The NO_2 concentrations at the occurrence time of the 4 peaks were all below 50 ppb. NO_2 often exceeded 50 ppb during the campaign, however, HONO stayed below 7 ppb throughout the whole campaign, except for the 4 cases studied in this work.

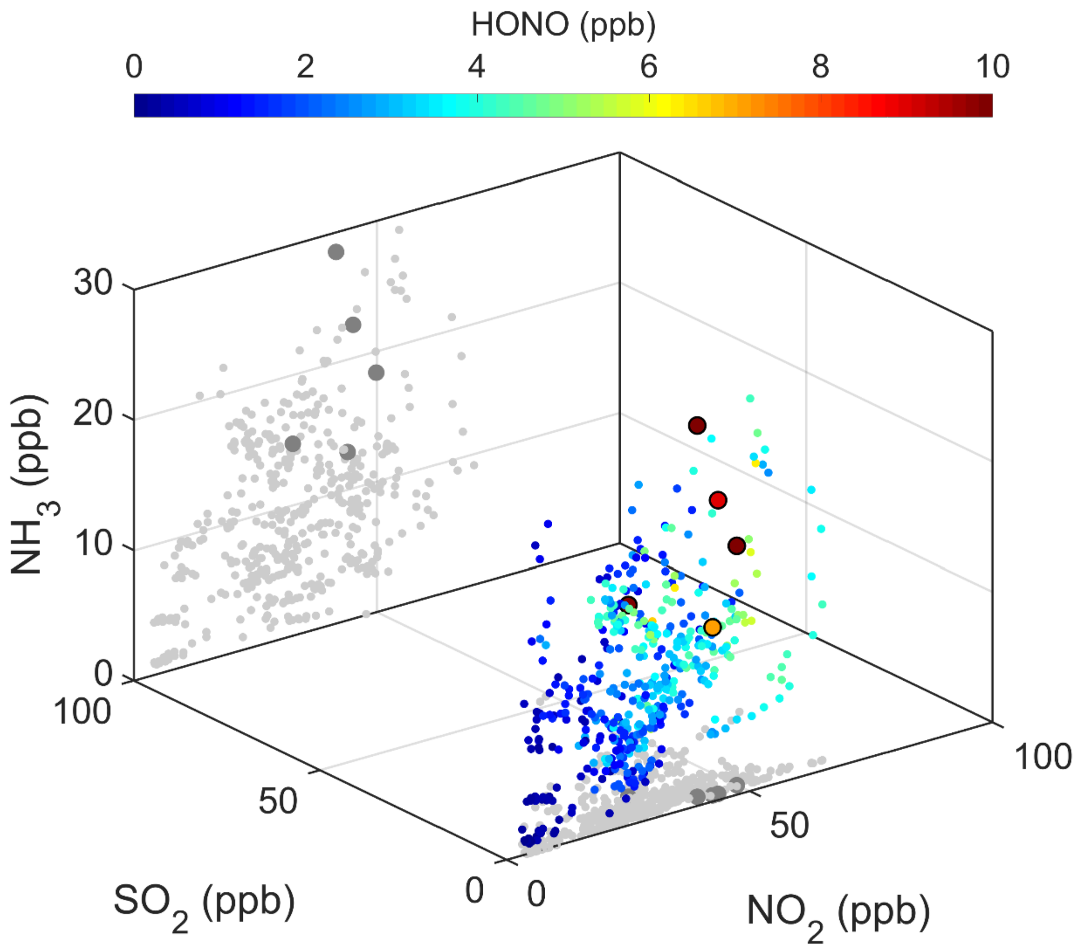

Figure 3 Variation of HONO with SO_2 (y-axis), NO_2 (x-axis) and NH_3 (z-axis) during 15th Oct. to 25th Nov. 2016, with the large dots indicating the data points with HONO exceeding 7 ppb

2. Line 213-214: "The O_3 concentration stayed near zero, which means that UV radiation was weak." This statement is clearly wrong. From the few NO data that the author disclose to the reader one can see that NO values are typically ranging from 20 to 100 ppb. With such high values, no wonder why O_3 remain low: it is clearly titrated by NO. One can understand that the lack of spectral radiometer measurements is an issue (see later) but O_3 data in a polluted environment can certainly not be used as a proxy for UV radiation strength.

Response:

We thank the reviewer for this valuable comment and agree that using O_3 as an indicator for UV radiation under such conditions is indeed not appropriate. As suggested by the reviewer in the following major comment, we used TUV calculation results to prove our point. During the case on the 14th Nov. 2016, the relative humidity decreased from 100% (10:00-11:00) to 85% (11:30), suggesting that this was a fog dissipation process. During 10:00 to 11:00, Gucheng was still under foggy conditions, with an estimated HONO lifetime (only considering its photolysis process) of 1.7 hours, proving that the photolysis process was relatively weak during the rapid increase of HONO. The estimated HONO lifetime rapidly decreased to 0.6 h by 12:00, resulting in accelerated HONO dissociation and OH production, explaining the rapid decrease of HONO concentrations.

The discussion in Line 213-214 was deleted and detailed discussions on the HONO photolysis were added in both Sect. 4.1 and Sect. 4.3 of the revised manuscript.

3. Line 226: Equation 1 is strongly oversimplified. On the HONO sinks side one clearly miss - photolysis that can certainly not be neglected. Even if radiation measurements are not available, the authors manage, later on in the paper, to evaluate some values that could be used here. Another approach would be to provide an upper limit evaluating the J value above haze using TUV for example (see Madronich et al, 1988 and Tie et al, 2003) - deposition can be taken into account by using as deposition velocity the value given by Stutz et al., 2002, for example. In

addition in the presence of hydrometeors, one clearly miss the loss processes onto/into haze droplets. On the HONO source side, may well identified processes are missing such as direct emission and heterogeneous HONO formation from conversion of NO_2 on ground surface and aerosol surfaces.

Response:

We thank the reviewer for the valuable suggestions in this comment. However, we believe there has been a little misunderstanding, which needs to be clarified. In this section, we tried to speculate if these observed HONO explosive growth events could have been caused by other known sources. In the second paragraph (line 224-236), we wanted to estimate if the homogenous oxidation of NO to HONO could be strong enough to produce such large amounts of HONO. Thus, Equation 1 was not meant to describe the net production of HONO based on all of its sources and sinks. It only describes the net HONO production via homogeneous gas phase reaction. The impact of direct emission is considered in the 3rd and 4th paragraph (line 233-251), which discuss the potential impact of vehicle and biomass burning emissions. The conversion of NO_2 on ground surface and aerosol surface is exactly what we are mainly discussing in the next paragraphs in this section (line 252-340). **We try to improve this section considering the reviewers suggestions and discuss all the known sources and sinks together to improve both the readability and scientific quality of the manuscript.** We calculated the following sources and sinks of HONO:

1) Gas phase homogeneous production of HONO:

$$P_{NO+OH}^{net} = k_{NO+OH}[NO][OH] - k_{HONO+OH}[HONO][OH], \qquad (1)$$

where diurnal variation of OH concentrations was inferred from Whalley et al. (2015), replacing OH under fog conditions with $1\text{x}10^5$ cm^{-3}).

2) Vehicle emissions: P_{emi}=Emission factor*$[NOx]_{vehicle}$, where the emission factor was assumed to be 1% (maximum emission factor of 0.8% used in Huang et al. (2017)) and the total observed NOx was attributed to vehicle emission to obtain an upper limit for the vehicle emission.

3) Heterogeneous conversion on aerosol and ground surface:

Typically, the conversion of NO_2 on aerosol and ground surface is parameterized as a linear function of NO_2 uptake coefficients and surface to volume ratios (surface area densities) (Xue et al., 2014;Li et al., 2018):

$P_{het}=(k_g+k_a)\times[NO_2]$, (2-1)

Ground: $k_g = \frac{1}{8} \cdot \vartheta_{NO2} \cdot \gamma_g \cdot \frac{S}{V}$ (2-2)

Aerosol: $k_a = \frac{1}{4} \cdot \vartheta_{NO2} \cdot \gamma_a \cdot S_a$ (2-3)

ϑ_{NO2} stands for the mean molecular speed, γ_g and γ_a for the uptake coefficient on ground and aerosol surface, S/V for the surface to volume ratio and Sa for the ambient aerosol surface area density. We estimate ground surface HONO production using a γ_g of $1e^{-6}$ during night time and $2e^{-5}$ during daytime and an S/V of 0.1 m^{-1}. The heterogeneous HONO production in aerosol and fog droplets were already calculated using a γ_a range of $1e^{-4}$ to $1e^{-3}$ as suggested by Li et al. (2018). Since the surface area density under fog conditions were not measured, we can only estimate that dHONO/dt during fog events would exceed 40 ppb/hour based on calculation results in Fig.S1. For non-fog conditions, we used the ambient aerosol surface area density calculated using the humidified nephelometer and $\gamma_a=1e^{-4}$ to further calculate the variation of the HONO production on aerosol surface.

4) Loss through photolysis:

$L_{pho}=J_{Hono}\times[HONO]$, (3)

where J_{HONO} was modelled using the TUV model, assuming AOD to vary with pH (see Table S1 in revised supplement).

Loss through dry deposition:

$L_{dep}=v_{dep}/H\times[HONO]$, (4)

where the dry deposition rate v_{dep} was assumed to be 0.3 cm s^{-1} according to Stutz et al. (2002) and the boundary layer height H was interpolated from ECWMF ERA-interim data (http://apps.ecmwf.int/datasets/data/interim-full-daily/).

Finally, the net production rate can be expressed as:

$$P_{HONO}^{net} = P_{NO+OH}^{net} + P_{het} + P_{emi} - L_{pho} - L_{dep} \qquad (6)$$

Fig. 4 displays the estimated production and loss of HONO via various routes, as well as the calculated and actually observed dHONO/dt during the 4th, 5th, 11th and 14th Nov. 2016. The estimated upper limit for vehicle emissions displays little variability during the day, with slight decreasing trends during the four events, proving that the observed HONO production could not have been caused by direct vehicle emissions. The net gaseous phase production of HONO (P_{hom}^{net}) contributed 0.15-0.18, 0.04-0.07, 0.27-1.04 and 0.25-1.53 ppb h^{-1} during the 4 case events, displaying little influence during fog events and more during haze events. However, the estimated P_{hom}^{net} was far from sufficient to explain the observed d[HONO]/dt. Dry deposition was typically high during the night within the shallow nocturnal boundary layer and decreased during the day with the increase of the boundary layer height. The calculated L_{dep} contributed 0.5-0.9, 0.4-0.6, 2.7-4.3 and 0.05-0.3 ppb h^{-1} to the loss of HONO. No significant decreases in L_{dep} were observed during the two fog events, while increases were detected during the cases on 11th and 14th Nov. Not only was the variation in L_{dep} unable to explain observed HONO productions, it further added to the discrepancy between observed and calculated d[HONO]/dt. During the four case events the J_{HONO} respectively increased from 0.7×10^{-4} to 2.5×10^{-4} s^{-1}, 1.6×10^{-4} to 2.4×10^{-4} s^{-1}, 0.03×10^{-4} to 1.4×10^{-4} s^{-1} and 1.6×10^{-4} to 4.4×10^{-4} s^{-1}, with L_{pho} contributing 0.9-8.9, 2.2-7.8, 0.03-5.5 and 0.8-26.4 ppb h^{-1} to the loss of HONO. J_{HONO} increased significantly by the end of the HONO growth events to 2.9×10^{-4}, 4.3×10^{-4}, 2.6×10^{-4} and 6.6×10^{-4} s^{-1}, respectively, suggesting that the rapid drop of HONO concentrations was high probably caused by the rapid photolysis. Overall, L_{pho} contributed most to the discrepancy between observed and calculated d[HONO]/dt.

Generally, the observed and calculated d[HONO]/dt agreed better with each other outside the HONO explosive growth periods, showing overestimations when aerosol liquid water contents were high, suggesting possible overestimation in the NO_2 uptake coefficient in the parameterization of P_{het}. This further suggests that the observed discrepancies in HONO production have mainly been caused by uncertainties in the heterogeneous formation estimates. The fact that HONO drastically increased while NO_2 varied little (9:30 to 11:30, 5th Nov. and 6:30 to 8:30, 11th Nov.) or hardly increased even under drastic increases of NO_2 (8:30 to 11:30, 14th Nov.), but displayed explosive growth with increasing NH_3, could not be explained by current known HONO sources (direct emission or gas phase reactions). Additionally, these rapid increasing HONO phenomena were all observed under foggy or high RH conditions, which further affirms the suspicion that the HONO increase was caused by heterogeneous conversion of NO_2.

The above results were added to the discussions in Sect. 4.1.

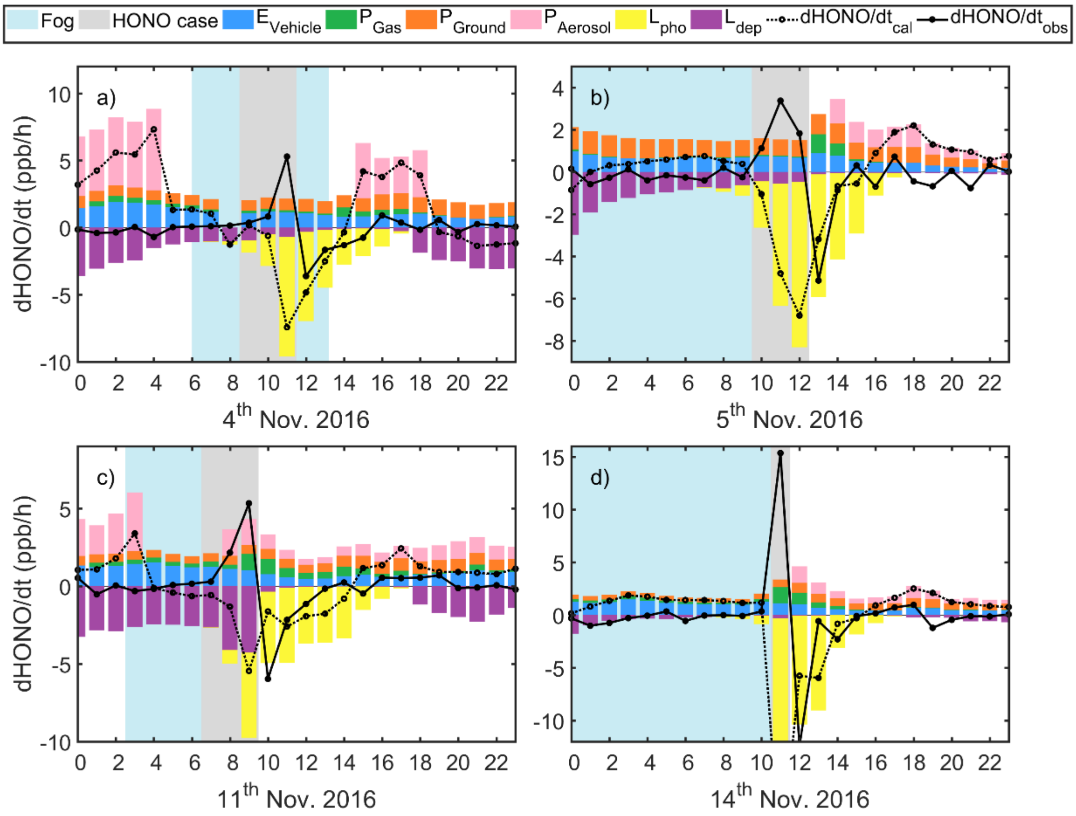

Figure 4 Estimated HONO emission from vehicles (blue), gas phase production (green), production on ground (orange) and aerosol surface (pink), loss through photolysis (yellow) and dry deposition (purple), as well as the calculated (dotted black) and actually observed (solid black) d[HONO]/dt on a) 4th, b) 5th, c) 11th and d) 14th Nov. 2016

4. Line 304-306 then line 326-329: In these section the photolysis of HONO is described being rapid (which is probably true) while it has been neglected earlier. I think the manuscript need reorganization to discuss more coherently the

photochemistry of HONO under these conditions.

Response:

We thank the reviewer for pointing that out. Sect. 4.1 has been reorganized and new results (already mentioned in previous comment) were added. Discussion on the HONO photolysis were also made for the other three cases in the revised manuscript in Sect.4.1: "During the four case events the J_{HONO} respectively increased from 0.7×10^{-4} to 2.5×10^{-4} s^{-1}, 1.6×10^{-4} to 2.4×10^{-4} s^{-1}, 0.03×10^{-4} to 1.4×10^{-4} s^{-1} and 1.6×10^{-4} to 4.4×10^{-4} s^{-1}, with L_{pho} contributing 0.9-8.9, 2.2-7.8, 0.03-5.5 and 0.8-26.4 ppb h^{-1} to the loss of HONO. J_{HONO} increased significantly by the end of the HONO growth events to 2.9×10^{-4}, 4.3×10^{-4}, 2.6×10^{-4} and 6.6×10^{-4} s^{-1}, respectively, suggesting that the rapid drop of HONO concentrations was high probably caused by the rapid photolysis. Overall, L_{pho} contributed most to the discrepancy between observed and calculated d[HONO]/dt."

Minor issues

1. Figure 2: it is somewhat disturbing that the figure does not displayed all the data acquired. In particular (but not only) the absence of NO and ozone data is clearly a problem. Furthermore, the use of "ppb" for aerosol composition is confusing: is it related to the whole volume of air? Is it related to the whole aerosol quantity. Please use more straightforward units here.

Response:

We included NO and O_3 concentrations in Figure 2 revised manuscript (see Fig. 5 below) according to the reviewer's suggestion. We also agree with the reviewer that the use of "ppb" as a unit for aerosol composition is confusing. The units in the text and in Figs. 2-4 in the revised manuscript were changed to "µg m^{-3}" instead (see Figs. 5-7 below).

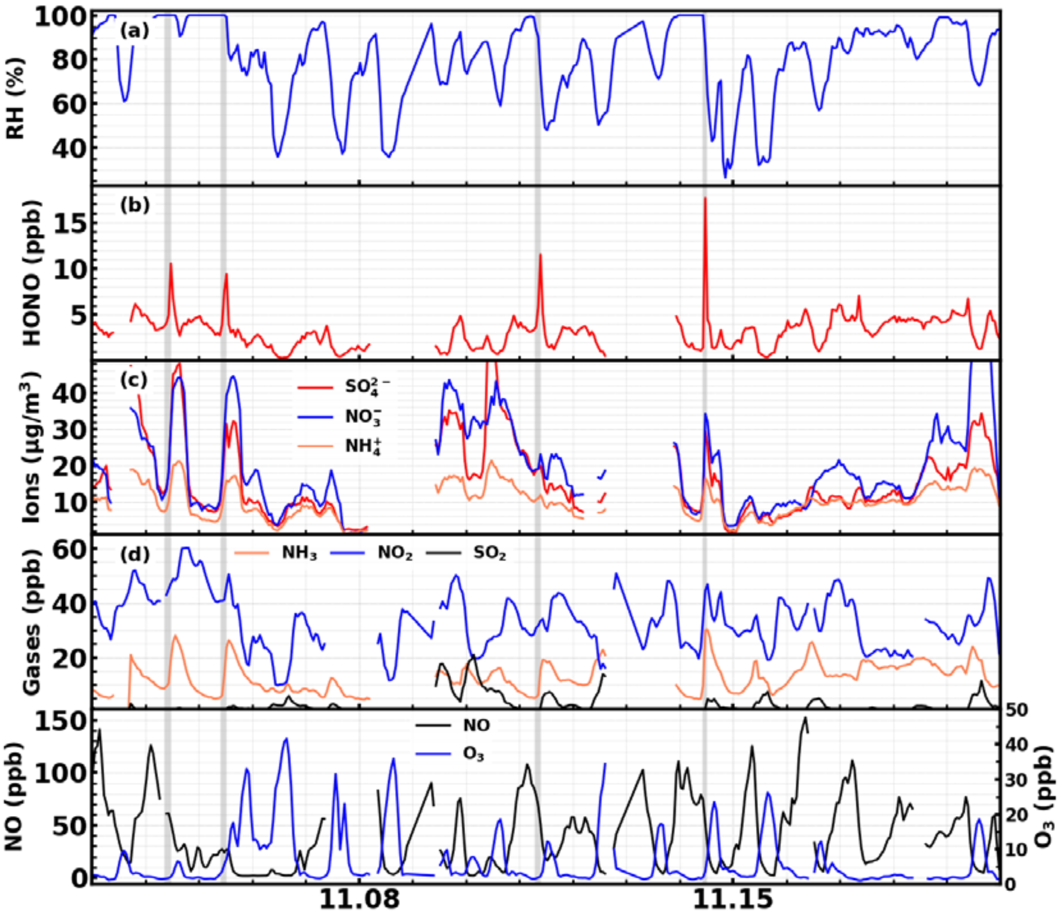

Figure 5. Time series of ambient **a)** RH; **b)** HONO; **c)** sulfate, nitrate, ammonium; **d)** NH_3, NO_3 and SO_2 during the observation period.

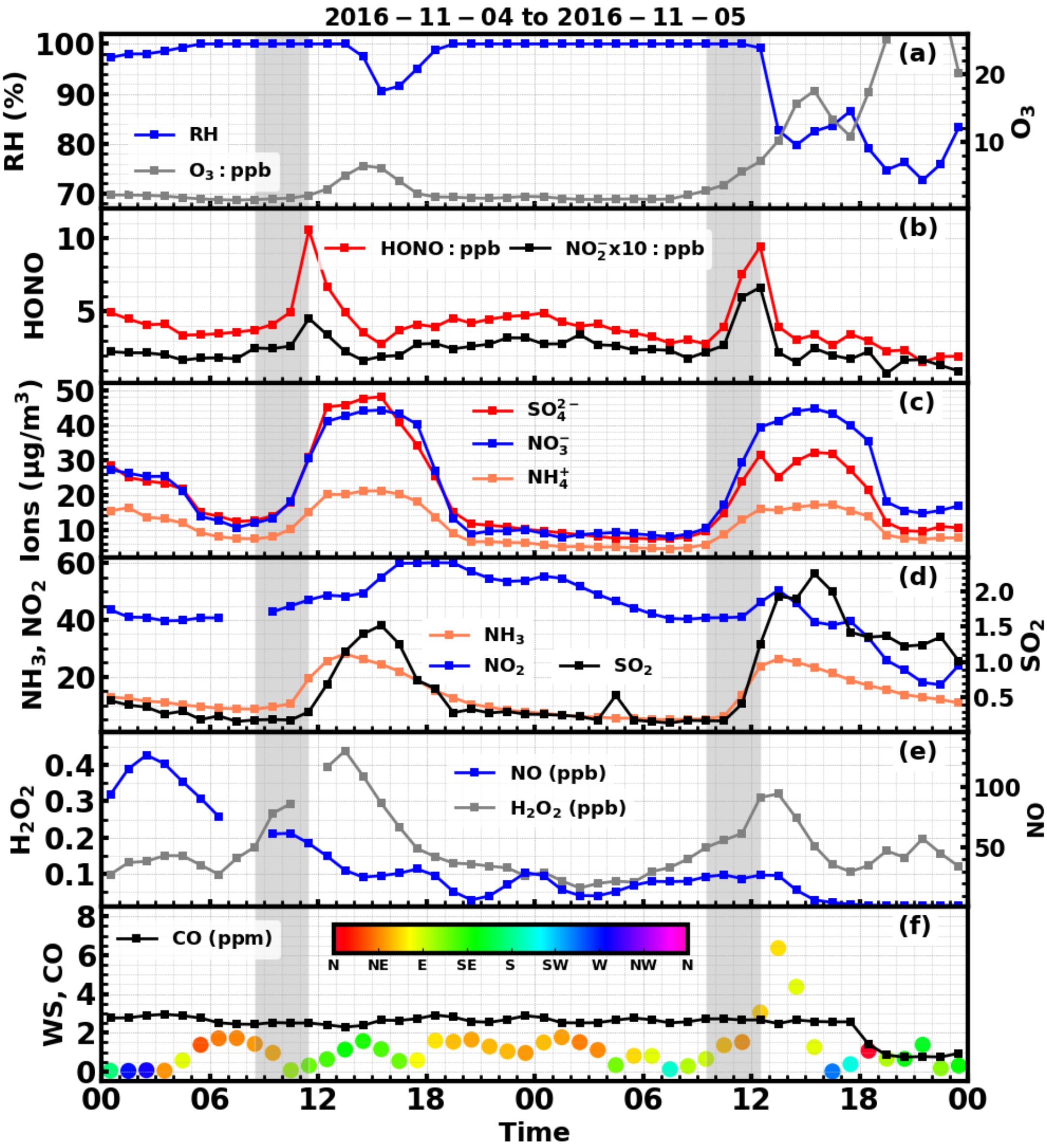

Figure 6 Time series of ambient **a)** RH,O_3, **b)**HONO, NO_2^-, **c)** SO_4^{2-}, NO_3^-, NH_4^+, **d)** NH_3, NO_2, SO_2, **e)** NO, H_2O_2, **f)** CO, wind speed and wind direction (colors of scatter points) from 11-04 to 11-05. Gray shaded areas represent periods of rapid increase of HONO.

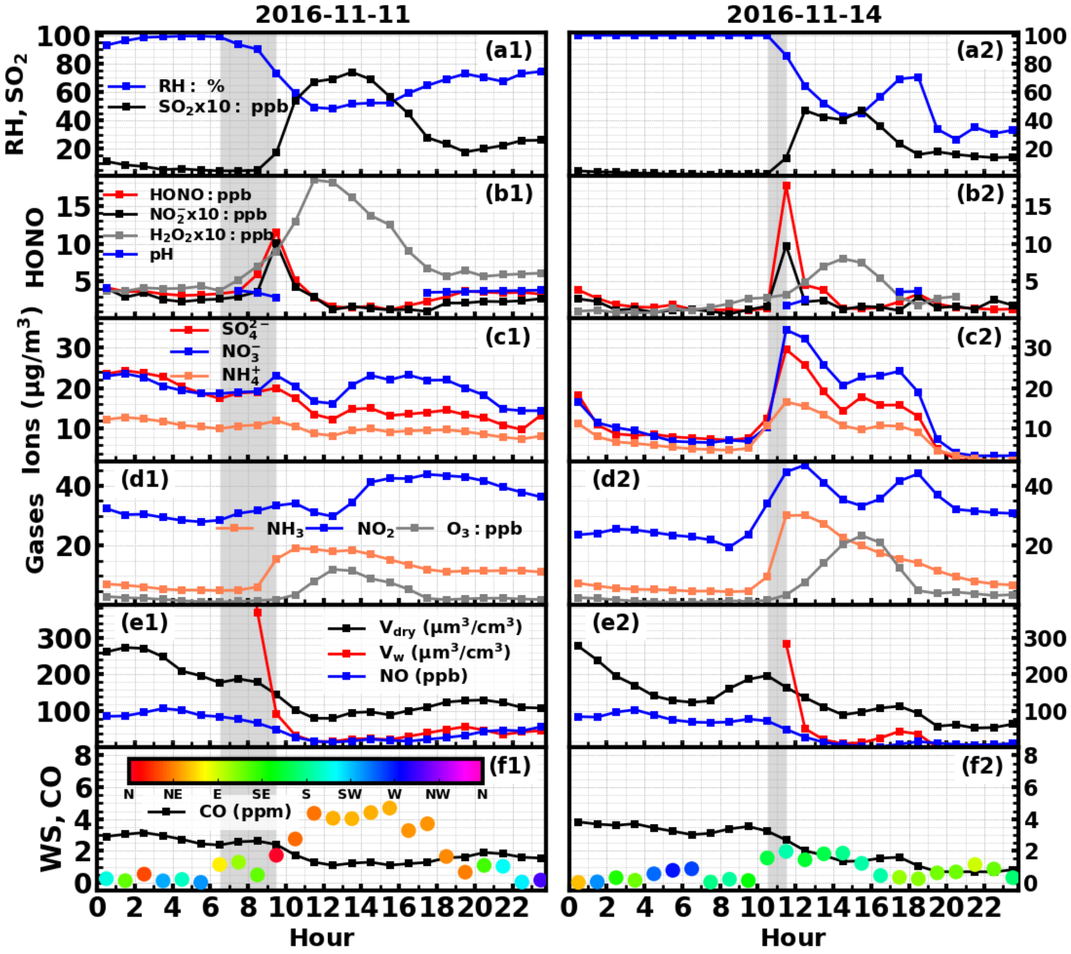

Figure 7 Time series of ambient **a)** RH, SO_2, **b)** HONO, NO_2^-, H_2O_2, aerosol pH, **c)** SO_4^{2-}, NO_3^-, NH_4^+,**d)** NH_3, NO_2, O_3, **e)** NO, volume concentrations of $PM_{2.5}$ in dry state (V_{dry}), volume concentrations of liquid water (V_w), **f)** CO, wind speed and wind direction during **1)** 11th Nov. 2016 and **2)** 14th Nov. 2016. Gray shaded areas represents periods of rapid increase of HONO.

2. Line 98 – 108: The experimental description of the instrument, the inlet and the protocol is insufficient.

Response:

We thank the reviewer for pointing it out and added more details to the experimental description on the instrument.

This part was revised as follows:

"During this field campaign, an In situ Gas and Aerosol Compositions Monitor (IGAC, Fortelice International Co.,Taiwan) was used for monitoring water-soluble ions (Na^+, K^+, Ca^{2+}, Mg^{2+}, NH_4^+, SO_4^{2-}, NO_3^-,NO_2^-, Cl^-) of $PM_{2.5}$ (particulate matter with aerodynamic diameter less than 2.5 μm) and trace gases including HONO, SO_2, NH_3, HCl, and HNO_3 with a time resolution of 1h. The IGAC system draws in ambient air through a PM10 inlet and passes the sample through a sharp-cut PM2.5 cyclone at a flowrate of 16.7 L/min. The total length of the stainless steel sampling line is approximately 2 m, with an inner diameter of 3.18 cm (1.25 inch), resulting in a residence time below 6 s, suggesting that underestimates in NH_3 possibly caused by adsorption on the stainless steel sampling tube as was proposed by Young et al. (2016) might be unimportant. A vertical annular denuder wetted with dilute H_2O_2 solution ($5x10^{-3}$ M) collects the trace gases and converts SO_2 rapidly to SO_4^{2-}, preventing SO_2 from reacting with NO_2 in the absorption solution to produce HONO artefacts. A scrub and impact aerosol collector under the denuder is mounted at an inclined angle to capture particles based on impaction after condensation growth. Two separate Ion Chromatographs are used to respectively analyze anions and cations for the gas and aerosol liquid extracts which were injected from the denuder and the aerosol collector once an hour. The detection limits are below 0.12 $\mu g/m^3$ and the background concentration of most water-soluble inorganic ions within the instrument were below 0.11 $\mu g/m^3$, only with SO_4^{2-} showing a background concentration of 1.10 $\mu g/m^3$ (Young et al., 2016). Under highly polluted conditions such as our site, these measurement uncertainties are fully acceptable. The instrument has shown good performance in the past, agreeing well with filter based samples (Liu et al., 2017). Standard LiBr solution was continuously added to the aerosol liquid extracts during the measurements, to ensure the sampling and analyzing process is stable. The swing amplitude was within the range of three standard deviation, confirming the stability of the ion analyzing system throughout the campaign. A mixed standard solution was diluted to perform multipoint calibrations (at 5, 10, 20, 50, 100, 200, 500 and 1000 ppb concentrations) at the beginning and at the end of the campaign for the ions Na^+, K^+, Ca^{2+}, Mg^{2+}, NH_4^+, Li^+, SO_4^{2-}, NO_3^-,NO_2^-, Cl^-, Br^-, with the R^2 of the calibrations reaching above 0.9999."

3. Line 120: The authors indicate the use of a NOx monitor 42CTL from thermo. It is not clear if this instrument is equipped with a Mo-based converter, a Blue light converter or both. In any case, the risk of interferences with HONO on the NO_2 and

> NOx channels are high (through the conversion of HONO on heated Mo – see Dunlea et al, 2007 for example - or through its photolysis by the blue light. During some part of this field campaign the HONO values can be as high as 20 % of NO_2. In this case it would be necessary to evaluate the cross-sensitivities of NO_2 and HONO in the configuration of the chemiluminescence monitor used.

Response:

We thank the reviewer for making a good point. The TE-42CTL NOx monitor at the Gucheng site is only equipped with a Mo-based converter, which means that HONO, PAN and HNO_3 can interfere with the NO_2 and NOx measurements. This we will clarify in our revised manuscript. During the entire campaign, the median value of HONO/NO_2 reaches 6.8%, while 90% of the data display HONO/NO_2 below 12.7%. The largest HONO/NO_2 were observed during the explosive HONO growth episodes in this study, which are shown in Fig.3. The NO_2 data measured by the TE-42C (red line) is compared against that subtracted by HONO (yellow line). Assuming all the HONO were converted to NO by the Mo-based converter, the actual NO_2 concentration would be similar to the yellow line in Figure 3, which only during the rapid HONO increase shows relatively larger deviation from the red line. Although there is indeed an impact of HONO on NO_2 measurements, NO_2 concentrations subtracted by HONO are still in excess, not limiting its conversion to HONO.

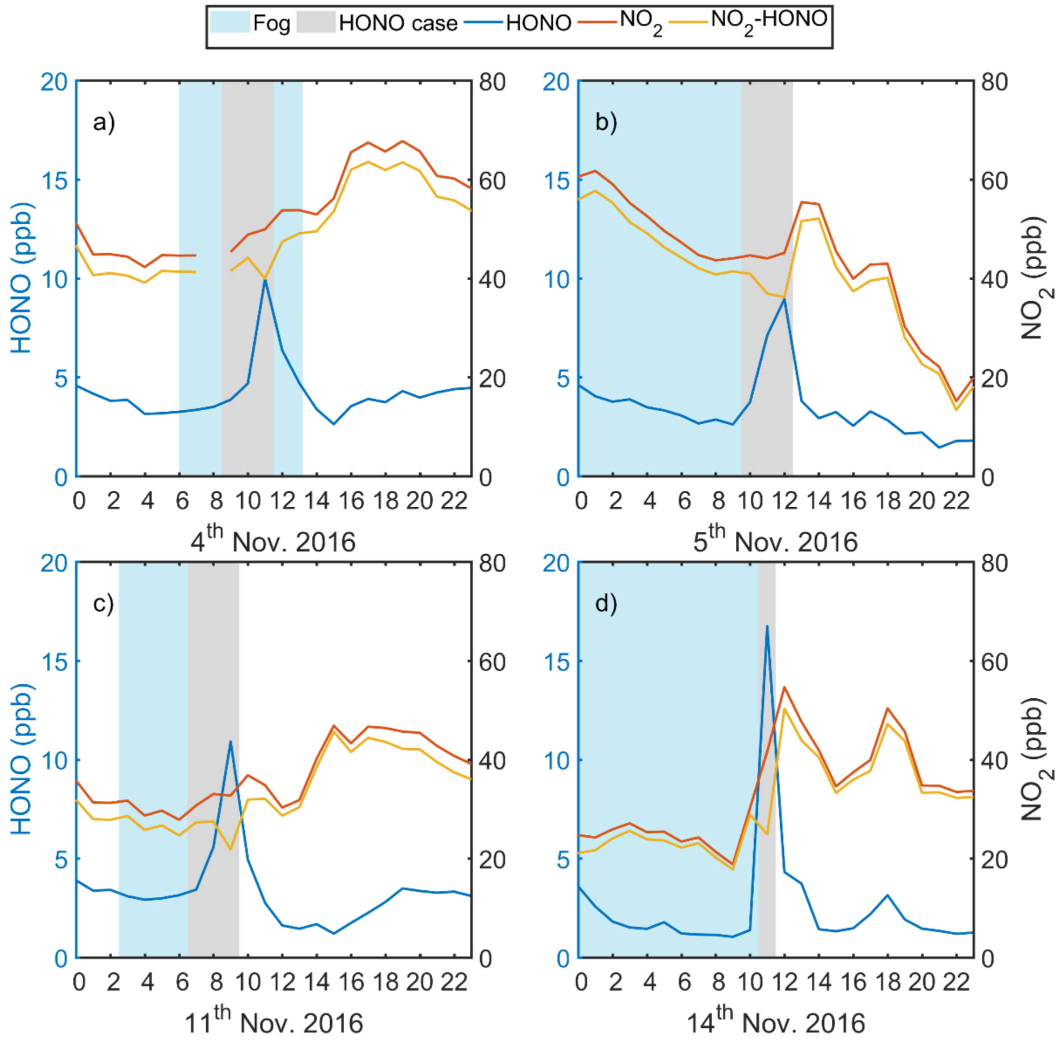

Figure 8 HONO, NO_2, NO_2-HONO concentrations on a) 4th, b) 5th, c) 11th and d) 14th Nov. 2016

4. Line 127: “wavelength” is misspelled

Response:

Thanks, correction made in the revised manuscript.

5. Line 229: The value of 10^6 radicals/cm^3 is taken as “typical for noontime haze condition” and later used in the equation 1. Even if the order of magnitude of this guess is probably not too wrong there is no reference provided. Furthermore, I don’t think that the scientific community have the necessary background to raise a “typical value” for these quite peculiar conditions. I would rather recommend to refer to published work such as Whalley et al, 2015 (field) or Tie et al, 2003 (large

scale modeling)

Response:

We thank the reviewer for the suggestion and have added the suggested reference by Whalley et al. (2015). The diurnal variation therein was used to estimate the diurnal variation of gas phase HONO production (see response to Major Comment #3).

6. Line 267-269: This statement is quite vague. Which anions are the authors referring to? More explanation are needed.

Response:

We added the following explanations to the introduction part, where this was first mentioned:

"Results of Yabushita et al. (2009) suggest that anions (such as Cl-, Br- and I-) greatly enhance the hydrolysis of NO_2 on water, and the NO_2 uptake coefficients of R2 can be enhanced several orders of magnitude by increasing electrolyte concentration."

References

Feng, T., Bei, N., Zhao, S., Wu, J., Li, X., Zhang, T., Cao, J., Zhou, W., and Li, G.: Wintertime nitrate formation during haze days in the Guanzhong basin, China: A case study, Environmental Pollution, 243, 1057-1067, https://doi.org/10.1016/j.envpol.2018.09.069, 2018.

Gu, J., Zhang, Y., Zeng, L., and Wen, M.: Evaluation of the Performance of a Gas and Aerosol Collector (GAC), Research of Environmental Sciences, 22, 16-22, DOI:10.13198/j.res.2009.01.18.gujw.002, 2009.

Huang, R.-J., Yang, L., Cao, J., Wang, Q., Tie, X., Ho, K.-F., Shen, Z., Zhang, R., Li, G., Zhu, C., Zhang, N., Dai, W., Zhou, J., Liu, S., Chen, Y., Chen, J., and O'Dowd, C. D.: Concentration and sources of atmospheric nitrous acid (HONO) at an urban site in Western China, Science of The Total Environment, 593-594, 165-172, https://doi.org/10.1016/j.scitotenv.2017.02.166, 2017.

Li, L., Hoffmann, M. R., and Colussi, A. J.: Role of Nitrogen Dioxide in the Production of Sulfate during Chinese Haze-Aerosol Episodes, Environmental Science & Technology, 52, 2686-2693, 10.1021/acs.est.7b05222, 2018.

Liu, M., Song, Y., Zhou, T., Xu, Z., Yan, C., Zheng, M., Wu, Z., Hu, M., Wu, Y., and Zhu, T.: Fine particle pH during severe haze episodes in northern China, Geophysical Research Letters, 44, 5213-5221, doi:10.1002/2017GL073210, 2017.

Meng, Z., Xu, X., Lin, W., Ge, B., Xie, Y., Song, B., Jia, S., Zhang, R., Peng, W., Wang, Y., Cheng, H., Yang, W., and Zhao, H.: Role of ambient ammonia in particulate ammonium formation at a rural site in the North China Plain, Atmos. Chem. Phys., 18, 167-184, 10.5194/acp-18-167-2018, 2018.

Nie, W., Ding, A. J., Xie, Y. N., Xu, Z., Mao, H., Kerminen, V. M., Zheng, L. F., Qi, X. M., Huang, X., Yang, X. Q., Sun, J. N., Herrmann, E., Petäjä, T., Kulmala, M., and Fu, C. B.: Influence of biomass burning plumes on HONO chemistry in eastern China, Atmos. Chem. Phys., 15, 1147-1159, 10.5194/acp-15-1147-2015, 2015.

Qiang, Y., Hang, S., Xin, L., YaFang, C., KeDing, L., Peng, C., JianWei, G., Song, G., Min, H., LiMin, Z., Tong, Z., and YuanHang, Z.: Daytime HONO formation in the suburban area of the megacity Beijing, China, Science China(Chemistry), 57, 1032-1042, 2014.

Stutz, J., Alicke, B., and Neftel, A.: Nitrous acid formation in the urban atmosphere: Gradient measurements of NO2 and HONO over grass in Milan, Italy, Journal of Geophysical Research: Atmospheres, 107, LOP 5-1-LOP 5-15, doi:10.1029/2001JD000390, 2002.

Su, H.: HONO: a study to its sources and impacts from field measurements at the sub-urban areas of PRD region, Peking University, Beijing, China, 2008.

Su, H., Cheng, Y. F., Shao, M., Gao, D. F., Yu, Z. Y., Zeng, L. M., Slanina, J., Zhang, Y. H., and Wiedensohler, A.: Nitrous acid (HONO) and its daytime sources at a rural site during the 2004 PRIDE-PRD experiment in China, Journal of Geophysical Research: Atmospheres, 113, doi:10.1029/2007JD009060, 2008.

Teng, X., Hu, Q., Zhang, L., Qi, J., Shi, J., Xie, H., Gao, H., and Yao, X.: Identification of Major Sources of Atmospheric NH3 in an Urban Environment in Northern China During Wintertime, Environmental Science & Technology, 51, 6839-6848, 10.1021/acs.est.7b00328, 2017.

Whalley, L. K., Stone, D., George, I. J., Mertes, S., van Pinxteren, D., Tilgner, A., Herrmann, H., Evans, M. J., and Heard, D. E.: The influence of clouds on radical concentrations: observations and modelling studies of HO_x during the Hill Cap Cloud Thuringia (HCCT) campaign in 2010, Atmos. Chem. Phys., 15, 3289-3301, 10.5194/acp-15-3289-2015, 2015.

Xie, Y., Ding, A., Nie, W., Mao, H., Qi, X., Huang, X., Xu, Z., Kerminen, V.-M., Petäjä, T., Chi, X., Virkkula, A., Boy, M., Xue, L., Guo, J., Sun, J., Yang, X., Kulmala, M., and Fu, C.: Enhanced sulfate formation by nitrogen dioxide: Implications from in situ observations at the SORPES station, Journal of Geophysical Research: Atmospheres, 120, 12679-12694, 10.1002/2015JD023607, 2015.

Xue, L. K., Wang, T., Gao, J., Ding, A. J., Zhou, X. H., Blake, D. R., Wang, X. F., Saunders, S. M., Fan, S. J., Zuo, H. C., Zhang, Q. Z., and Wang, W. X.: Ground-level ozone in four Chinese cities: precursors, regional transport and heterogeneous processes, Atmos. Chem. Phys., 14, 13175-13188, 10.5194/acp-14-13175-2014, 2014.

Yang, W., Cheng, P., Tian, Z., Zhang, H., Zhang, M., and Wang, B.: Study on HONO pollution characteristics and daytime unknown sources during summer and autumn in Guangzhou, China, China Environmental Science, 37, 2029~2039, 2017.

Young, L.-H., Li, C.-H., Lin, M.-Y., Hwang, B.-F., Hsu, H.-T., Chen, Y.-C., Jung, C.-R., Chen, K.-C., Cheng, D.-H., Wang, V.-S., Chiang, H.-C., and Tsai, P.-J.: Field performance of a semi-continuous monitor for ambient PM2.5 water-soluble inorganic ions and gases at a suburban site, Atmospheric Environment, 144, 376-388, https://doi.org/10.1016/j.atmosenv.2016.08.062, 2016.

NH_3-promoted hydrolysis of NO_2 induces explosive growth in HONO

Wanyun Xu[1], Ye Kuang[2,*], Chunsheng Zhao[3], Jiangchuan Tao[2], Gang Zhao[3], Yuxuan~~-~~ Bian[4], Wen Yang[5], Yingli Yu[3], Chuanyang Shen[3]–, Linlin Liang[1], Gen Zhang[1], Weili Lin[6], Xiaobin Xu[1]

[1] State Key Laboratory of Severe Weather, Key Laboratory for Atmospheric Chemistry, Institute of Atmospheric Composition, Chinese Academy of Meteorological Sciences, Beijing, 100081, China.

2 Institute for Environmental and Climate Research, Jinan University, Guangzhou, China.

[3] Department of Atmospheric and Oceanic Sciences, School of Physics, Peking University, Beijing, China

[4] State Key Laboratory of Severe Weather, Chinese Academy of Meteorological Sciences, Beijing, 100081, China

[5] State Key Laboratory of Environmental Criteria and Risk Assessment, Chinese Research Academy of Environmental Sciences, Beijing, 100081, China

[6] College of Life and Environmental Sciences, Minzu University of China, Beijing, 100081, China

Corresponding author: Ye Kuang (kuangye@jnu.edu.cn)

Abstract

The study of atmospheric nitrous acid (HONO), which is the primary source of OH radicals, is crucial to atmospheric photochemistry and heterogeneous chemical processes. The heterogeneous NO_2 chemistry under haze conditions was pointed out to be one of the missing sources of HONO on the North China Plain, producing sulfate and nitrate in the process. However, controversy exists between various proposed mechanisms, mainly debating on whether SO_2 directly takes part in the HONO production process and what roles NH_3 and the pH value play in it. In this paper, never before seen explosive HONO production (maximum rate: 16 ppb~~/hour~~ h^{-1}) was reported and evidence was found for the first time in field measurements during fog episodes (usually with $4<$pH~~>5~~<6) and haze episodes under high relative humidity (~~usually with~~ pH~~<5~~≈ 4), that NH_3 was the key factor that promoted the hydrolysis of NO_2, leading to explosive growth of HONO and nitrate under both high and lower pH conditions. The results also suggest that SO_2 ~~does not directly take~~takes minor or insignificant part in the HONO formation during fog and haze events, but was indirectly oxidized upon the photolysis of HONO through subsequent radical mechanisms. Aerosol hygroscopicity significantly increased with the rapid inorganic secondary aerosol formation further promoting the HONO production~~.~~ as a positive feedback. For future

photochemical and aerosol pollution abatement, it is crucial to introduce effective NH_3 emission control measures, since the NH_3-promoted NO_2 hydrolysis is a large daytime HONO source, releasing large amounts of OH radicals upon photolysis, which will contribute largely to both atmospheric photochemistry and secondary aerosol formation.

1 Introduction

Nitrous acid (HONO) plays a vital role in atmospheric chemistry due to the fact that its photolysis is a major source (Michoud et al., 2014;Kleffmann et al., 2005) of hydroxyl radical (OH) which determines the atmospheric oxidative capacity and plays crucial role in tropospheric chemistry in processes such as the ozone formation, the degradation of volatile organic compounds and the secondary aerosol formation (Cheng et al., 2016;Wang et al., ~~2016b~~2016). Hence, the source study of nitrous acid (HONO) is of crucial importance for the understanding of the tropospheric chemistry, for chemistry and climate modelling and for developing effective pollution control strategies (Lu et al., 2018).

The North China Plain (NCP) is troubled by the persistent complex air pollution with high loadings of both photochemical pollutants and particulate pollution (Zheng et al., 2015;Ran et al., 2011) and the simultaneous mitigation of the two types of pollution has encountered trouble due to the nonlinear dependence of ozone on NOx ~~(Xing et al., 2018)~~(Xing et al., 2018). Unknown daytime sources of HONO caught attention during the past few years (Michoud et al., 2014;Liu et al., 2014;Su et al., 2011) and results from a recent study indicate that an additional missing source is required to explain more than 50% of observed HONO concentration in the daytime in Western China ~~(Huang et al., 2017)~~(Huang et al., 2017). Results from several recent studies demonstrate that intense heterogeneous conversion of NO_2 to HONO on particle surfaces might be a significant source of HONO (Liu et al., 2014;Cui et al., 2018).

Two main HONO heterogeneous production pathways involving aerosol water and NO_2 were proposed. In light of drastic decrease of solar radiation during severe haze events and rich ammonia conditions on the NCP, the first pathway hypothesized that NO_2 (g) dissolved in aerosol water at aerosol pH > 5.5 rapidly formed HONO while oxidizing HSO_3^- (aq) to sulfate. The stoichiometry of this mechanism is as follows (Cheng et al., 2016;Wang et al., ~~2016a~~2016):

$2NO_2$ (aq) + HSO_3^- (aq) + H_2O (l) ~~=>~~ → $2H^+$ + HSO_4^- (aq) + $2NO_2^-$ (aq). (R1)

Based on this mechanism, good agreement between modelled and observed sulfate formation rates were achieved. However, the assumption that the pH of ambient aerosols can reach beyond 5.5 is a debatable issue. Results from several most recent studies indicate that the pH of ambient aerosols fall in the range of 3-5 in most cases (Ding et al., 2018;Liu et al., 2017a;Song et al., 2018). Given this, it was proposed that HONO and NO_2^- were produced in the hydrolysis process of NO_2, releasing OH radicals upon photolysis, which indirectly oxidize SO_2 to sulfate ~~(Li et al., 2018b)~~(Li et al., 2018b):

$2NO_2$ (g) + H_2O (l) ~~=>~~ → H^+ + NO_3^- (aq) + HONO. (R2)

Results of ~~Yabushita et al. (2009) suggest that anions~~Yabushita et al. (2009) suggest that anions (such as Cl^-, Br^- and I^-) greatly enhance the hydrolysis of NO_2 on water, and the NO_2 uptake coefficients of R2 can be enhanced several orders of magnitude by increasing electrolyte concentration. The ambient aerosol particles in the boundary layer are in aqueous phase under high RH (Liu et al., 2017b) and the aerosol or fog water is not pure with different dissolved anions (Wu et al., 2018;Lu et al., 2010). Therefore, HONO and nitrate formed through this mechanism should be independent of aerosol acidity, and should be primarily affected by the aerosol surface area density, aerosol liquid water content and NO_2 concentration ~~(Li et al., 2018b)~~(Li et al., 2018b). Moreover, recent theoretical simulations have proposed a HONO formation mechanism involving NO_2 and water and have identified that NH_3 can promote the hydrolysis of NO_2 (Li et al., 2018a) (R2). Despite of this, no direct evidence from field observations were available in this paper to support their findings.

Although the proposed HONO formation mechanisms are all heterogeneous reactions of NO_2, the details of how SO_2, pH and NH_3 are involved in heterogeneous formation are still under debate ~~(Li et al., 2018b)~~(Li et al., 2018b) and a clear mechanism is still missing in current models to explain both the daytime concentration of observed HONO and the secondary inorganic aerosol formation. Measurements of HONO are rare and simultaneous observations of HONO and aerosol physical and chemical characteristics are lacking to thoroughly analyze or directly support the aerosol heterogeneous HONO formation mechanisms involving NO_2. In this paper, we present for the first time simultaneous measurements of HONO, sulfate and nitrate as well as other precursor gases, oxidants and meteorological parameters during both fog and haze episodes under high ambient RH. Fog water pH is usually greater than 5.5 in eastern China (Safai et al., 2008;Lu et al., 2010), while calculations in this work and previous studies collectively indicate a moderately acidic condition (4<pH<5) for fine particles in northern China winter haze. The observational results unveil that NH_3 is the key factor that promotes the hydrolysis of NO_2, resulting in explosive formation of HONO, nitrate and sulfate.

2 Site description and instruments

From 15th Oct. to 25th Nov. 2016, a field campaign intended to study sulfate formation was conducted at the Ecological and Agricultural Meteorology Station (39°09′N, 115°44′E) of the Chinese Academy of Meteorological Sciences. The site is partly composed of experimental farmland and is also surrounded by farmland and small residential towns (nearest town ~1.5 km). It is located between Beijing (~ 100km) and Baoding (~40km), two megacities on the North China Plain (Fig. 1). During this field campaign, an In situ Gas and Aerosol Compositions Monitor (IGAC, Fortelice International Co.,Taiwan) was used for monitoring water-soluble ions (Na^+, K^+, Ca^{2+}, Mg^{2+}, NH_4^+, SO_4^{2-}, NO_3^-,NO_2^-, Cl^-) of $PM_{2.5}$ (particulate matter with aerodynamic diameter less than 2.5 µm) and trace gases including HONO, SO_2, NH_3, HCl, and HNO_3 with a time resolution of 1h. The IGAC system draws in ambient air through a PM10 inlet and passes the sample through a sharp-cut PM2.5 cyclone at a flowrate of 16.7 L~~/~~ min~~.~~$^{-1}$. The total length of the stainless steel sampling line is approximately 2 m, with an inner diameter of 3.18 cm (1.25 inch), resulting in a residence time below 6 s, suggesting that underestimates in NH_3 possibly caused by adsorption on the stainless steel sampling tube as was proposed by Young et al. (2016) might be unimportant. A vertical annular denuder wetted with dilute H_2O_2 solution (5x10^{-3} M) collects the trace gases~~.~~ and converts SO_2 rapidly to SO_4^{2-}, preventing SO_2 from reacting with NO_2 in the absorption solution to produce HONO artefacts. A scrub and impact aerosol collector under the denuder is mounted at an inclined angle to capture particles based on impaction after condensation growth. Two separate Ion Chromatographs are used to respectively analyze anions and cations for the gas and aerosol liquid extracts which were injected from the denuder and the aerosol collector once an hour. The detection limits are below 0.12 µg~~/m^3~~ m^{-3} and the background concentration of most water-soluble inorganic ions within the instrument were below 0.11 µg~~/m^3~~ m^{-3}, only with

SO_4^{2-} showing a background concentration of 1.10 μg~~/m^3 (Young et al., 2016). Under highly polluted conditions such as our site~~ m^{-3} (Young et al., 2016). Considering the severe pollution state the NCP is under, these measurement uncertainties are fully acceptable. The instrument has shown good performance in the past, agreeing well with filter based samples ~~(Liu et al., 2017a)~~(Liu et al., 2017a). Standard LiBr solution was continuously added to the aerosol liquid extracts during the measurements, to ensure the sampling and analyzing process is stable. The swing amplitude was within the range of three standard deviation, confirming the stability of the ion analyzing system throughout the campaign. A mixed standard solution was diluted to perform multipoint calibrations (at 5, 10, 20, 50, 100, 200, 500 and 1000 ppb concentrations) at the beginning and at the end of the campaign for the ions Na^+, K^+, Ca^{2+}, Mg^{2+}, NH_4^+, Li^+, SO_4^{2-}, NO_3^-,NO_2^-, Cl^-, Br^-, with the R^2 of the calibrations reaching above 0.9999. A comparison between NH_3 observed by IGAC and by an economical NH_3 analyser (LGR, DLT-100, details see Meng et al. (2018)) yielded an overall slope of 0.91 with R=0.63 (Fig.S1a). A better comparison result (slope of 1.03, R=0.74) would be obtained if data associated with RH≥80 were excluded (Fig.S1b). The overestimation of LGR instruments compared to denuder based instruments has also been reported in Teng et al. (2017), suggesting possible interference of water vapor on NH_3 measurements. As can be seen in Fig.S2, both instruments captured the same the diurnal variation of NH_3 during the four case episodes in this study, which proves that the IGAC instrument was able to capture the overall variation trends of NH_3. Since both instruments have their uncertainties, we decided to use the NH_3 measured by the IGAC instrument for better consistency with the other data.

NOx and CO were observed using commercial instruments from Thermo Electronics (Model 42CTL and 48CTL), while the Aerolaser AL2021 H_2O_2-monitor was used to measure H_2O_2 concentrations. The ambient RH, temperature, wind speed and wind direction were observed using an automatic weather station. The dry state particle number size distributions (PNSDs) in the diameter range of 3nm to 10μm, were jointly measured by a scanning mobility particle size spectrometer (SMPS) and an Aerodynamic Particle Sizer (APS, TSI Inc., Model 3321). The ambient aerosol liquid water concentrations were calculated based on measurements of a three-~~wavlength~~wavelength humidified nephelometer system (Kuang et al., 2018). The aerosol hygroscopicity parameter κ (Petters and Kreidenweis, 2007) is calculated using the method proposed by ~~Kuang et al. (2017)~~Kuang et al. (2017).

3 Observed simultaneous rapid increase of HONO, nitrate and sulfate

The time series of HONO, sulfate, nitrate and ammonium and precursor gases, meteorological parameters and other parameters are shown in Fig. 2. During this observation period, HONO concentration ranged from 0.31 to 17.6 ppb (ranged from 0.3 to 6.0 ppb during most periods) with an average of 3.0 ppb. The HONO/NO_2 ratio ranged from 0.03 to 0.75 with an average of 0.18, which is higher than the average HONO/NO_2 ratio previously observed in China (Liu et al., 2014;Cui et al., 2018). NO_2 concentration ranged from 7.5 to 60.1 ppb with an average of 32.0 ppb. NH_3 concentration ranged from 0.05 to 30 ppb with an average of 12.3 ppb. Four rapid HONO formation events were identified in Fig.2, two under foggy conditions and the other two under high RH conditions.

3.1 Explosive growth of HONO during fog episodes

Two dense fog episodes with rapid HONO increase were observed for the first time in China, occurring on the 4th and 5th Nov. 2016. From satellite images (Fig. 1) it can be seen that on the 5th Nov., a wide area of the NCP was shrouded by fog before noon (about 11:30) including the observation site, however, the fog area reduced in the afternoon (about 13:30) and dissipated near the observation site. The evolution of the fog-shrouded area during these two days was also observed by a geostationary satellite (http://www.eorc.jaxa.jp/ptree/index.html). These two fog episodes offer us a great opportunity to study the hydrolysis process of NO_2 (R2) and the role of SO_2 in heterogeneous HONO production in fog water (R1), which usually show pH above 5.5 (Safai et al., 2008;Lu et al., 2010).

The time series of simultaneously observed meteorological parameters, concentrations of nitrate, ammonium, sulfate and their precursor gases SO_2, NO_2, NO and NH_3, as well as atmospheric oxidants such as O_3, H_2O_2 and other parameters including CO, which is indicative of transport processes during the two days with fog episodes are shown in Fig. 3. From 0:00 (Beijing local time) on the 4th Nov., the ambient RH continuously increased and reached 100% near 5:00, and lasted about 8.5 hours before it dropped below 100% near 13:30. However, at 15:30, the ambient RH began to rise again and reached 100% near 19:30, and then sustained until 12:00 on the 5th Nov. The latter fog episode lasted about 18.5 hours.

During the first fog episode, the rapid increases of HONO, nitrate, sulfate and ammonium were observed from 8:50 to 11:30 (Case1). HONO increased from 3.6 ppb to 10.6 ppb, with the most rapid increase occurring around 11:00 at a rate of 5.5 ppb~~/~~ h^{-1}. During the HONO increasing period, the variation characteristics of related trace gases and other parameters are as follows. NH_3 concentration increased slowly at first and then increased drastically near 11 am (10 ppb~~/~~ h^{-1}). SO_2 concentration remained almost constant at first and then increased from near 0.25 ppb to 0.4 ppb. NO_2 concentration increased continuously with a small magnitude, while NO concentration increased first and then decreased. H_2O_2 concentration is continuously increasing, but O_3 concentration remained near zero. CO concentration remained almost constant (~2.5 ppm), suggesting that there was no evident plume transport during this process. Wind speed was less than 2 m~~/~~ s^{-1}, and dropped almost to 0 ~~-~~m~~/~~ s^{-1} when HONO concentration dramatically increased, further supporting the fact that the drastic increase was not caused by transport processes. Ammonium, nitrate and sulfate concentration steadily increased from ~~10.~~7~~, ~~.5, 13.2, 13.7 μg m^{-3}~~.5 ppb~~ to ~~20.5, 12~~14.3, 30.4, 31.0~~, 7.9 ppb~~ μg m^{-3}, respectively. A noticeable increase in nitrite was also observed, when HONO increased most rapidly. It should be noted that the cutting diameter of the IGAC instrument is 2.5 μm, which means that observed concentrations only represent the variation of inorganics ions in aerosol water, and that of fog droplets were not included.

During the second fog episode, HONO, nitrate, sulfate and ammonium started to increase rapidly from 9:30 and reached a plateau near 12:30, when the fog started to dissipate (Case2). HONO increased from 3 ppb to 9.5 ppb, with the fastest increase occurring near 11:00 at a rate of 3.5 ppb~~/~~ h^{-1}. Variation characteristics of other parameters are as follows. NH_3 concentration increased steadily from 5 ppb to 24 ppb. SO_2 concentration increased steadily from 0.25 ppb to 1.25 ppb. NO_2 concentration remained almost constant at the very beginning (near 40 ppb) and then increase slightly, while NO concentration remained almost constant (near 30 ppb) throughout the entire fog period. H_2O_2 concentration increased slightly at first and then rose rapidly towards the end of the fog period. O_3 concentration increased very slightly. CO concentration remained also near constant (~3 ppm). Wind speed was steady and less than 2 m~~/~~ s^{-1} at the beginning, however, began to increase quickly at noon. Ammonium, nitrate and sulfate concentration steadily grew from ~~11.7, 6.7~~8.1, 17, 3.8~~ ppb~~ μg m^{-3} to ~~22,~~ 15.~~5~~3, 39.3, 8~~ ppb~~.0 μg m^{-3}, respectively. The variation of nitrite was very similar to that of HONO. The variation of wind speed demonstrate that at the very beginning of the HONO increase, the air mass was relatively stagnant, but became windy when the fog dissipated.

3.2 Explosive growth of HONO during haze episodes with high RH conditions

The two periods with rapid HONO increase under high RH conditions occurred on the 11th and 14th Nov., respectively. The time series of simultaneously observed meteorological parameters, concentrations of nitrate, ammonium, sulfate and their precursor gases SO_2, NO_2, NO and NH_3, as well as oxidants including O_3, H_2O_2 and other parameters such as CO concentration, aerosol volume concentration in dry state and aerosol liquid water content during the two days are shown in Fig.4.

On the 11th Nov., HONO started rising from 6:30 (3.4 ppb) and came to a halt at 9:00 (11.5 ppb) (Case 3). The quickest increase of HONO occurred near 9 o'clock with a rate of 5.6 ppb~~/~~ h^{-1}. The key features of other parameters are introduced in the following. The ambient RH decreased rapidly (from foggy condition to near 75%). NH_3 increased slowly at first and then grew rapidly. NO_2 increased slowly and SO_2 remained low. The total volume concentration of $PM_{2.5}$ was decreasing. Ammonium, nitrate and sulfate concentrations increased very slowly at first and then evident increase was observed in ammonium and nitrate. The decrease in dry state volume concentration of $PM_{2.5}$ demonstrate that the air mass is not quite steady due to transport or boundary layer processes. The slight increase of nitrate and sulfate despite the drop in total $PM_{2.5}$ concentration suggest that the nitrate and sulfate produced during the increasing process of HONO outgrew those lost to boundary layer mixing and transport.

On the 14th Nov., HONO increased drastically near 11:00, reaching 17.6 ppb at 11:30 (16.1 ppb~~/~~ h^{-1}) and then dropped promptly to 4 ppb at 12:30 (Case 4). This phenomenon took place when the fog dissipated and the ambient RH abruptly dropped to near 85%. Key variation features of other parameters are as follows. NH_3 increased rapidly from 9.7 ppb to 30 ppb. NO_2 concentration was increasing quickly, while SO_2 concentration remained low. The concentration of sulfate and nitrate also increased quickly. Volume concentration of $PM_{2.5}$ was decreasing, indicating that even more sulfate and nitrate were formed than the observed growth in their concentrations. ~~The O_3 concentration stayed near zero, which means that UV radiation was weak. After the quick formation of HONO, O_3 concentration began to rise, indicating the increase in UV radiation intensity.~~ The photolysis of HONO was high probably the cause for its drastic decrease. Note that the HONO was not increasing during the period where only NO_2 increased rapidly and NH_3 varied little.

4 Discussions

4.1 ~~Discussions on the~~ HONO ~~formation mechanism~~budget analysis

In these four rapid HONO increasing episodes, the maximum HONO growth rates (~~dHONO/~~d[HONO]/dt) all exceed 5 ppb~~/~~ h~~,~~$^{-}$, and even reach beyond 16 ppb~~/~~ h^{-1}. Such high HONO growth rates as observed in this study were not yet reported in literature.

~~The homogeneous reaction of NO with OH is an important source of HONO~~In this section, we discuss whether these HONO formation events can be explained by current known mechanisms and which mechanisms are determining the variation of HONO.

The net HONO production rate can be estimated by accounting for all the currently known sources and sinks using the following equation:

$$P_{HONO}^{net} = P_{emi} + P_{hom}^{net} + P_{het} - L_{pho} - L_{dep}, \qquad \text{(Eq.1)}$$

where P_{emi} is the total emission rate of HONO, P_{hom}^{net} the net HONO production in homogenous gas phase reactions, P_{het} the HONO produced via heterogeneous reactions, L_{pho} the loss of HONO due to photolysis and L_{dep} the loss of HONO due to deposition.

Previous studies have shown that HONO can be emitted through biomass burning and vehicles (Nie et al., 2015;Huang et al., 2017). Biomass burning contributes to HONO mainly by increasing particle surface area and NO_2 conversion efficiency (Nie et al., 2015). Under foggy conditions, surface area was not the limiting factor to the NO_2 conversion. During the haze events, particle surface area was decreasing due to decreasing humidity and aerosol water content. Hence, the variation of surface area cannot explain the observed HONO increases. According to the mapped fire spots on the days of the HONO events (Fig.S3), there was no fire within 20 km distance to the site. K^+ is often used as an indicator for biomass burning. The average K^+ concentration during the whole campaign ranged from 0.022 to 5.95 μg m^{-3}, with an average of 1.28 μg m^{-3}. The K^+ level during the four events were 1.39, 1.08, 1.51 and 1.54 μg m^{-3}, respectively, showing no evident sign of biomass burning. Hence, only vehicle emissions were considered in this study.

Vehicle emissions can be estimated using the following equation:

$$\mathrm{P}_{vehicle} = \mathrm{R}_{emission} \times [\mathrm{NO}_x]_{vehicle}, \qquad \text{(Eq.2)}$$

where $R_{emission}$ is the vehicle emission ratio and $[NO_x]_{vehicle}$ the NOx concentration from vehicle emissions. The NO/NOx ratio during the HONO increasing episodes ranged from 0.37 to 0.76, suggesting that the air masses were relatively aged compared to freshly emitted air mass from exhaust (NO/NOx>0.9). ~~P_{NO+OH}^{net}~~Here, $P_{vehicle}$ is estimated assuming all the measured NOx came from vehicle emissions and an emission ratio of 1%, which is higher than the upper limit of 0.8% used in Huang et al. (2017), to obtain an upper limit for vehicle emissions.

HONO can be formed in gas phase reactions of NO with OH radicals and is lost through direct reactions with OH radicals. The net production of HONO via homogeneous reactions can be estimated using the equation:

$$P_{hom}^{net} = k_{NO+OH}[NO][OH] - k_{HONO+OH}[HONO][OH], \qquad \text{(Eq. ~~1~~3)}$$

where ~~k_{NO+OH}~~k_{NO+OH} (7.2×10^{-12} cm^{-3} s^{-1}) and ~~$k_{HONO+OH}$~~ $k_{HONO+OH}$ (5.0×10^{-12} cm^{-3} s^{-1}) are the rate constants of the reactions of NO and HONO with OH, at 298 k, respectively (Li et al., 2012). ~~Using an OH concentration of 1×10^{6} cm^{-3}, typical for noontime haze conditions, the estimated homogeneous production rate are 2.04, 0.79, -0.33 and -0.37 ppb/h for the episodes on 4th, 5th, 11th and 14th Nov., respectively, showing little variability or decreases during the increase of HONO. Clearly, homogeneous oxidation of NO cannot explain the observed HONO variations~~The diurnal variation of OH concentrations was inferred from Whalley et al. (2015), replacing OH under fog conditions with $1\text{x}10^{5}$ cm^{-3}.

Heterogeneous conversion of NO_2 on aerosol and ground surface is considered a major source for HONO. However, the detailed mechanism (R1 or R2?) is still under debate and different studies have shown a large variability in the range of estimated NO_2 uptake coefficient. Typically, the conversion of NO_2 on aerosol and ground surface is parameterized as a linear function of NO_2 uptake coefficients and surface to volume ratios (surface area densities) (Xue et al., 2014;Li et al., 2018b):

$$P_{het} = (k_g + k_a)[NO_2], \qquad \text{(Eq.4-1)}$$

$$k_g = \frac{1}{8} \cdot \vartheta_{NO2} \cdot \gamma_g \cdot \frac{S}{V}, \qquad \text{(Eq.4-2)}$$

$$k_a = \frac{1}{4} \cdot \vartheta_{NO2} \cdot \gamma_a \cdot S_a, \qquad \text{(Eq.4-3)}$$

where ϑ_{NO2} stands for the mean molecular speed, γ_g and γ_a for the uptake coefficient on ground and aerosol surface, S/V for the surface to volume ratio and S_a for the ambient aerosol surface area density. For NO_2 conversion on ground surface, γ_g is assumed to be 1×10^{-6} during nighttime and 2×10^{-5} during daytime and S/V is assumed to be 0.1 m^{-1} as in Vogel et al. (2003). Since no measurements of fog droplet surface areas were made in this experiment, we use a γ_a range of

1×10^{-4} to 1×10^{-3} as suggested by Li et al. (2018b) and a wide range of surface area densities to account for both aerosol and fog conditions. Additionally, for non-fog conditions, the ambient aerosol surface area density calculated using the simultaneously measured PNSD and aerosol hygroscopicity parameter derived from measurements of a humidified nephelometer system and $\gamma_a=1\times10^{-4}$ is applied to further calculate the variation of the HONO production on aerosol surface.

HONO loss through photolysis reactions were calculated as:

$$L_{pho} = J_{HONO}[HONO], \qquad \text{(Eq.5)}$$

where JHONO was modelled using the TUV radiative transfer model (version 5.3, http://www2.acom.ucar.edu/modeling/tuv). The required single scattering albedo and aerosol angstrom exponent were estimated using simultaneously measured PNSD and BC measurements (Kuang et al., 2015), while the 550nm aerosol optical depth (AOD) was assumed to vary with RH (Table S1).

Loss through dry deposition was estimated using equation 6:

$$L_{dep} = \frac{v_{dep}}{H}[HONO], \qquad \text{(Eq.6)}$$

where the dry deposition rate v_{dep} was assumed to be 0.3 cm s^{-1} according to (Stutz et al., 2002) and the boundary layer height H was interpolated from ECWMF ERA-interim data (http://apps.ecmwf.int/datasets/data/interim-full-daily/).

The comparison between the calculated HONO net production rate and actually measured HONO variation rate (d[HONO]/dt) is displayed in Fig. 5. The estimated upper limit for vehicle emissions displays little variability during the day, with slight decreasing trends during the four events, proving that the observed HONO production could not have been caused by direct vehicle emissions. The net gaseous phase production of HONO (P_{hom}^{net}) contributed 0.15-0.18, 0.04-0.07, 0.27-1.04 and 0.25-1.53 ppb h^{-1} during the 4 case events, displaying little influence during fog events and more during haze events. However, the estimated P_{hom}^{net} was far from sufficient to explain the observed d[HONO]/dt. Dry deposition was typically high during the night within the shallow nocturnal boundary layer and decreased during the day with the increase of the boundary layer height. The calculated L_{dep} contributed 0.5-0.9, 0.4-0.6, 2.7-4.3 and 0.05-0.3 ppb h^{-1} to the loss of HONO. No significant decreases in L_{dep} were observed during the two fog events, while increases were detected during the cases on 11th and 14th Nov. Not only was the variation in L_{dep} unable to explain observed HONO productions, it further added to the discrepancy between observed and calculated d[HONO]/dt. During the four case events the J_{HONO} respectively increased from 0.7×10^{-4} to 2.5×10^{-4} s^{-1}, 1.6×10^{-4} to 2.4×10^{-4} s^{-1}, 0.03×10^{-4} to 1.4×10^{-4} s^{-1} and 1.6×10^{-4} to 4.4×10^{-4} s^{-1}, with L_{pho} contributing 0.9-8.9, 2.2-7.8, 0.03-5.5 and 0.8-26.4 ppb h^{-1} to the loss of HONO. J_{HONO} increased significantly by the end of the HONO growth events to 2.9×10^{-4}, 4.3×10^{-4}, 2.6×10^{-4} and 6.6×10^{-4} s^{-1}, respectively, suggesting that the rapid drop of HONO concentrations was high probably caused by the rapid photolysis. Overall, L_{pho} contributed most to the discrepancy between observed and calculated d[HONO]/dt.

Generally, the observed and calculated d[HONO]/dt agreed better with each other outside the HONO explosive growth periods, showing overestimations when aerosol liquid water contents were high, suggesting possible overestimation in the NO_2 uptake coefficient in the parameterization of P_{het}. This further suggests that the observed discrepancies in HONO production have mainly been caused by uncertainties in the heterogeneous formation estimates. ~~The NO/NOx ratio during the HONO increasing episodes ranged from 0.37 to 0.76, suggesting that the air masses were relatively aged compared to freshly emitted air mass from exhaust (NO/NOx>0.9). Even if we assume all the measured NOx came from vehicle emissions and an emission ratio of 10%, which is higher than the upper limit of 8% used in Huang et al. (2017) (Huang et al., 2017), the contribution of vehicle emissions to HONO would be in the range of 0.97 to 1.09, 0.63 to 0.83, 0.73 to 1.16 and 0.9 to 1.15 ppb during the episodes on 4th, 5th, 11th and 14th Nov., respectively. Even if the emission ratio were underestimated, NOx decreased during these events with the increase in HONO, which proves that the observed HONO variation could not have been caused by direct vehicle emissions.~~

~~Recent studies also suggest biomass burning to be an important HONO source, mainly by increasing particle surface area and NO2 conversion efficiency (Nie et al., 2015). Under foggy conditions, surface area is not the limiting factor to the NO_2 conversion. During the haze events, particle surface area was decreasing due to decreasing humidity and aerosol water content. Hence, the variation of surface area cannot explain the observed HONO increases. According to the mapped fire spots on the days of the HONO events (Fig. S2), there was no fire within 20 km distance to the site. K^+ is often used as an indicator for biomass burning. The average K+ concentration during the whole campaign ranged from 0.022 to 5.95 μg/m3, with an average of 1.28 μg/m3. The K+ level during the four events were 1.39, 1.08, 1.51 and 1.54 μg/m3, respectively, showing no evident sign of biomass burning.~~

The fact that HONO drastically increased while NO_2 varied little (9:30 to 11:30, 5th Nov. and 6:30 to 8:30, 11th Nov.) or hardly increased even under drastic increases of NO_2 (8:30 to 11:30, 14th Nov.), but displayed explosive growth with increasing NH_3, ~~cannot~~could not be explained by current known HONO sources (direct emission or gas phase reactions). ~~These~~Additionally, these rapid increasing HONO phenomena were all observed under foggy or ~~under~~ high RH conditions, which ~~leads us to suspect~~further affirms the suspicion that the HONO increase was caused by heterogeneous conversion of NO_2. ~~Was it R1, R2 or another mechanism that led to the explosive growth of HONO?~~

~~Based on results from Wang et al. (2016a) and Cheng et al. (2016), R1 is more likely to happen during fog episodes or under NH_3 neutralized conditions (3,4). While R1 might be able to explain the formation of sulfate and HONO, it cannot explain that of nitrate. The observed molar increase of nitrate were always larger than that of sulfate, usually exceeding twice the amount of sulfate. In addition, pH values during the rapid HONO increasing period under high RH conditions (estimated from ISORROPIA with the forward mode and metastable assumption (Song et al., 2018), Fig. 4) were continuously below 5, further demonstrating that R1 is unlikely to happen under such conditions.~~

~~Laboratory experiments demonstrated that anions greatly enhance NO_2 uptake on water~~

4.2 Heterogeneous HONO formation mechanism

As manifested in Sect. 4.1, the unknown HONO source and the overestimates in HONO production were both linked to our limited understanding on the heterogeneous HONO formation mechanism. In this section, we try to evaluate the relative contribution of the currently known heterogeneous HONO formation pathways (R1 and R2) and reveal the reason for their limitations in explaining the observed HONO growth.

To evaluate which process (R1 or R2) was dominating the heterogeneous production of HONO, we assume that HONO was produced in aerosol and fog water simultaneously via R1 and R2. Since measurements of fog liquid water content or fog droplet surface area density were not made, we cannot directly quantify the absolute HONO production in fog. However, we can make a few assumptions to compare the relatively HONO contribution via R1 and R2. First, it was assumed that the observed sulfate production (d[SVI]/dt) was caused by the reaction of SO_2 with H_2O_2, O_3, NO_2, transition metal ions (TMI: Fe^{3+} and Mn^{2+}). Calculations were performed according to Cheng et al. (2016), using the same pH dependent TMI concentrations and the actually measured SO_2, H_2O_2, O_3 and NO_2 concentrations (Table S2). For the two fog episodes on 4th and 5th Nov. 2016, the mean diameter of fog droplets was assumed to be 7.0 µm and the liquid water content was assumed to be 0.3 g m^{-3} according to Shen et al. (2018). For the haze episodes on the 11th and 14th Nov. 2016, the mean aerosol diameter under ambient conditions was estimated to be 0.65-1.22 and 0.9 µm, while the liquid water content was calculated to decrease from 3.4×10^{-4} to 7.8×10^{-5} g m^{-3} on the 11th Nov and assumed to be 0.01 g m^{-3} on the 14th Nov. during the transition from fog to haze. The sulfate production rate and relative contribution of each oxidation pathway to the total sulfate production rate was obtained and depicted in Fig.6. For the two fog episodes, assuming pH=6, the estimated average sulfate production rates are 11.7 and 31.6 µg m^{-3} h^{-1} approximately 4 times of that observed within $PM_{2.5}$, which might be an underestimation, considering the liquid water content of fog droplets are at least a magnitude higher than that of aerosols. For the two haze episodes, using the pH values estimated using ISORROPIA (forward mode and metastable assumption (Song et al., 2018)), the estimated average sulfate production rates are 0.06 and 1.8 µg m^{-3} h^{-1}, about 10% of that observed within $PM_{2.5}$. Following the calculations of Cheng et al. (2016), we have considered the influence of ionic strength on the reaction rates and set constraints on the maximum ionic strength (I_{max}), which might have caused underestimations for all reaction routes, since the calculated ionic strength commonly exceeded I_{max}. Underestimated transition metal ion concentrations may also be partly responsible for the underpredicted sulfate production, since the TMI catalysis route has recently be pointed out to be the dominant SO_2 heterogeneous oxidation pathway {Shao, 2019 #2155}. Additionally, there also might be other neglected SO_2 oxidation pathways, which will lead to overestimates in the sulfate fraction produced by the NO_2 oxidation pathway. Therefore, we can only yield an upper limit for the HONO production rate of R1:

$$\frac{d[HONO]}{dt}_{R1} = 2 \times frac_{SO_2+NO_2} \times \frac{d[SVI]}{dt}_{obs}, \qquad \text{(Eq.7)}$$

where $frac_{SO_2+NO_2}$ is the contribution fraction of the NO_2 oxidation pathway to the total sulfate production. Note that the calculated HONO production rate can only represent the production within $PM_{2.5}$.

By further assuming that all the observed nitrate production ($d[NO_3^-]/dt$) was caused by reaction R2 and by the reaction of NO_2 with OH radicals (k_{NO_2+OH}=3.2×10^{-12} cm^3 s^{-1}), the HONO production rate of R2 would be:

$$\frac{d[HONO]}{dt}_{R2} = \frac{d[NO_3^-]}{dt}_{obs} - k_{NO_2+OH}[NO_2][OH]. \qquad \text{(Eq.8)}$$

The contribution fraction of the two reactions to the heterogeneous HONO production in aerosol and fog liquid water content can be calculated by:

$$f_{R1} = \frac{d[HONO]}{dt}_{R1} \Big/ \frac{d[HONO]}{dt}_{R1+R2} \text{ and} \qquad \text{(Eq.9-1)}$$

$$f_{R2} = \frac{d[HONO]}{dt}_{R2} \Big/ \frac{d[HONO]}{dt}_{R1+R2}. \qquad \text{(Eq.9-2)}$$

Assuming the pH of fog droplets falls within the range of 4 to 6, f_{R2} was estimated to range from range from 75.5 to 99.5% and from 81.2 to 99.5% during the 4th and 5th Nov. 2016, respectively. For the two haze events on 11th and 14th Nov., the f_{R2} corresponding to the pH values modelled by ISORROPIA would be 98.2% and 97.3%.

These results suggest that, reaction R2 is the dominant contributor to the heterogeneous HONO production, while R1 is more important under high pH conditions. Under the assumed upper limit of pH, R1 can contribute up to 24.5%, 18.8% to the observed HONO growth during the fog events. This is in accordance with results from ~~(Yabushita~~Wang et al~~., 2009;Li et al., 2018b~~. (2016)~~, which suggests that R2 is more likely to occur in fog water that is rich in anions. The concentration of NO_2 as well as the surface area density of fog droplets should be~~ and Cheng et al. (2016), which suggested that R1 was more likely to happen during fog episodes or under NH_3 neutralized conditions (3,4). For the two haze events, R1 contributed very little (1.8% and 2.7%) to the observed HONO growth.

Since R2 seems to be the dominant contributor to the observed HONO production, it is important to evaluate whether the parameterizations in current literature can accurately describe the HONO production process of R2. The HONO production rate of R2 is typically parameterized as in Eq.4, where the NO_2 concentration and the surface area density of fog droplets/aerosol particles are the controlling factors of the NO_2 uptake, as opposed to the pH of the water droplets~~.~~ (Li et al., 2018b;Yabushita et al., 2009). Based on the reactive uptake coefficient of NO_2 (γ_{NO_2}) ~~in Yabushita et al. (2009), we have~~ in Yabushita et al. (2009) and Li et al. (2018b), we have calculated the HONO production rate of R2 under different conditions (~~see~~ Fig.~~S1~~S4). During foggy conditions, the HONO production rate should be higher than 1~~-~~ ppb~~/(~~ (ppb~~-~~ NO_2·h~~).~~)$^{-1}$. The NO_2 concentration during the two fog episodes ranged between 40 to 50~~-~~ ppb, therefore, the HONO production rate ~~should be~~ would have been higher than 40 ppb~~/h during the observed fog periods according to the results in Fig.S1~~ h^{-1}. However, no rapid increase of HONO was observed unless NH_3 was simultaneously increasing. ~~This result indicates~~As already mentioned before, under hazy conditions, P_{het} significantly overestimated the HONO production when relative humidity was high and large ambient aerosol surface area densities were observed (Fig5), while it failed to reproduce the growth in HONO on the morning of the 11th Nov. 2016. These results indicate that R2 is missing the important impact of NH_3 in the heterogeneous HONO production and that the ~~currently used~~ γ_{NO_2} range is at least overestimated when NH_3 is not abundant enough.

Recent theoretical simulation results ~~(Li et al., 2018a)~~ ascertain that NH_3 can promote the hydrolysis of NO_2 and contribute to HONO formation via R2~~.~~ (Li et al., 2018a). This conclusion is consistent with the observed phenomena that HONO only increased rapidly when NH_3 was simultaneously increasing. Considering the influence of NH_3 and sulfate on the aerosol pH, under our observed NH_3 concentration range, NH_3 has negligible impact on pH values (Guo et al., 2017), especially under high RH conditions. This further proves that the NH_3-promoted hydrolysis of NO_2 is independent of the pH value.

~~So what role does SO_2 play in the HONO formation and what caused the rapid formation of sulfate? Li et al. (2018b) pointed out that NO_2 can oxidize S(IV) indirectly via free radical mechanism (the involved reactions RS1 to RS5 proposed in Li et al. (2018b) are listed in the supplement). The key step of the proposed S(IV) oxidation pathway is the photolysis of HONO to produce OH (RS1). Produced OH can oxidize S(IV) to form bisulfate or sulfate through reaction RS2 and produce HO_2. HO_2 can react with NO to produce NO_2, or react with itself to produce H_2O_2. Is the radiation during fog and haze events strong enough to photo dissociate the produced HONO and release large amounts of OH radicals? Diurnal evolutions of the lifetime of HONO (only considering the photolysis process) under different aerosol optical depth (AOD) and different cloud optical depth conditions are presented in Fig.5, which were calculated using the j-values simulated by the TUV radiative transfer model (version 5.3, http://www2.acom.ucar.edu/modeling/tuv, the required single scattering albedo and aerosol angstrom exponent were estimated using simultaneously measured PNSD and BC measurements~~

~~(Kuang et al., 2015). The results in Fig.5a demonstrate that for AOD (550nm)=1.0, the lifetime of HONO quickly drops below 1 hour after sunrise and is less than 0.5 hour at noontime. The AOD at 550 nm observed near 13:30 by the MODIS (Moderate resolution Imaging Spectroradiometer) Aqua satellite on the 14th November is 0.7, thus, the drastic decrease of HONO on the 14th November can be well explained by its rapid photolysis and the amount of OH radicals released must be even greater than the drop in HONO concentrations, since HONO was simultaneously produced via NO_2 hydrolysis. During Case 1 and 3, HONO began to decrease when NH_3 was still increasing. The reason might be that the UV radiation at that point was already strong enough to photolyze HONO quickly, which lead to the drastic drop in HONO concentrations (The diurnal evolution of lifetime of HONO under different cloud optical depth conditions are depicted in Fig.5b). O_3 started to increase quickly as HONO began to decrease, which is an indirect evidence of the increasing UV radiation. The increase in H_2O_2 during the increase of HONO in the two fog episodes, where O_3 concentration stayed near zero, might be an indirect evidence of the HO_2 production and occurrence of RS2. The formed H_2O_2 can also oxidize S(IV) to form sulfate via heterogeneous processes, even more efficient than the OH radical oxidation in the gas phase under high RH conditions. In this way, the simultaneous formation of HONO, sulfate and nitrate can be well explained and it becomes clear that SO_2 does not participate in the heterogeneous HONO production process.~~

Another phenomenon worth noting is that, in Case 3, HONO was increasing rapidly even under the drastic decrease in ambient RH, which demonstrates that the impact of NH_3 on HONO formation should be even more important than that of aerosol liquid water content. However, the hydrolysis of NO_2 needs water to be involved, thus, the importance of water content under different conditions remains to be elucidated.

To further investigate the acceleration effect of NH_3 on the hydrolysis of NO_2, we have examined the correlations between the NO_2-to-HONO (HONO/NO_2 ratio), NO_2-to-NO_3^- (NO_3^-/NO_2 ratio) conversion efficiencies and the NH_3 concentration during the entire field campaign (Fig.~~6~~7). Note that only data points during nighttime (18 pm to 6 am) and with ambient RH ~~Higher~~higher than 80% are ~~shown~~displayed in Fig.~~6.~~ 7. Daytime data were excluded, because HONO would quickly photolyze as soon as sunlight ~~is~~was available~~, even~~. Even if there was rapid HONO production, the corresponding increase of HONO might not be ~~observed~~observable due to its quick photolysis. The reason for only including data with ambient RH higher than 80% is

~~because~~that the quick hydrolysis of NO_2 requires water to be involved. However, the overall hygroscopicity of ambient aerosols during this field campaign ~~is~~was relatively low~~ (~~, with an average hygroscopicity parameter κ ~~is~~of 0.14, and the volume contribution of liquid water to the total volume concentrations of ambient aerosols was quite low when ambient RH is below 80% (Kuang et al., 2018)~~ and the volume contribution of liquid water to the total volume concentrations of ambient aerosols is quite low when ambient RH is below 80% during this field campaign. Details on the volume contribution of liquid water to the total volume of ambient aerosols can be referred to Kuang et al. (2018)~~. The correlation coefficient between $HONO/NO_2$ ratio and the NH_3 concentration reaches 0.68, while that between NO_3^-/NO_2 ratio and NH_3 concentration only reaches 0.48, since the source of NO_3^- is much more complicated than that of HONO. These results have further verified that NH_3 promotes the NO_2 hydrolysis and HONO production. The correlation of $HONO/NO_2$ to NH_3 is highly nonlinear, $HONO/NO_2$ increases rapidly with NH_3 when NH_3 reaches above 10 ppb.

4.~~2 Diurnal variations of ~~3 Feedback between HONO formation and inorganic secondary aerosol formation~~ and aerosol hygroscopicity determined by NH_3~~

~~According to the discussions in Sect.4.1, NH_3 promotes the hydrolysis of NO_2, producing HONO and nitrate. During daytime, HONO photolysis further produces OH and results in significant formation of sulfate. ~~According to the discussions in Sect.4.2, NH_3 promotes the hydrolysis of NO_2, producing nitrate and most of the observed HONO. However, the connection between the NH_3 promoted hydrolysis and the simultaneous rapid sulfate production remains unexplained. As was already discussed in Sect.4.2, the sulfate production rate calculated based on currently known SO_2 oxidation pathways largely underestimates the observed sulfate growth, indicating that there might be neglected oxidation pathways. Li et al. (2018b) pointed out that NO_2 can oxidize S(IV) indirectly via free radical mechanism (the involved reactions RS1 to RS5 proposed in Li et al. (2018b) listed in the supplement). The key step of the proposed S(IV) oxidation pathway is the photolysis of HONO to produce OH radicals (RS1). OH can oxidize S(IV) to form bisulfate or sulfate through reaction RS2 and produce HO_2. HO_2 can react with NO to produce NO_2, or react with itself to produce H_2O_2. As was depicted in Fig.5, the radiation during the fog/haze events was already strong enough to photolyze the produced HONO and release OH radicals at the same rates as L_{pho} in Sect. 4.1, indicating there was strong OH production, especially near the end of the events. For the two fog events, no AOD measurements were available. Assuming AOD=2.5 for foggy conditions, the lifetime of HONO (only considering the photolysis process) were estimated to decrease from 4.2 to 1.1 h, 1.7 to 1.1 h during the growth of HONO and to drop to 1.0 and 0.7 h by the time of the drastic decreases in HONO. In the haze event on the 11th Nov., AOD measurements were also not available due to cloud coverage, however, sensitivity study shows that the calculated HONO lifetime are much more sensitive to the AOD as opposed to the COD values (increasing 3.1 and 0.4 h per 0.1 increase in AOD and COD, Fig.S5). The HONO lifetime dropped from 2.0 h (by the time of the HONO peak) to 1.1 h (by time of the HONO decrease). During the case on the 14th Nov. 2016, the relative humidity decreased from 100% (10:00-11:00) to 86% (11:30), suggesting that this was a fog dissipation process. The HONO lifetime was estimated to be 1.7 h between 10:00 to 11:00, proving that the photolysis process was relatively weaker during the rapid increase of HONO. The estimated HONO lifetime rapidly decreased to 0.6 h by 12:00, resulting in accelerated HONO dissociation and OH production. The increase in H_2O_2 observed during and after the increase of HONO, might be an indirect evidence of the HO_2 production and occurrence of RS2. The observed H_2O_2 concentrations were much higher than the assumptions of 0.01 ppb made in Cheng et al. (2016), which was also pointed out by Ye et al. (2018). Under the assumed pH range for fog and the calculated pH range for aerosol, the estimated sulfate production was dominated by the SO_2 oxidation via H_2O_2 (Fig.6). This indicates that both the calculated and the yet unexplained sulfate production were linked to the photolysis of HONO.

NH_3 promoted the hydrolysis of NO_2, producing HONO and nitrate. HONO easily photolyzes releasing OH radicals, which further converted to HO_2 and H_2O_2. The highly oxidative free radicals and H_2O_2 collaboratively boosted the formation of sulfate. Hence, diurnal variations of NH_3 should have exerted significant influences on the diurnal variations of HONO and inorganic aerosol chemical components~~.~~ (sulfate, nitrate and ammonium, SNA). The average diurnal variations of NO_2, NH_3, HONO as well as SO_2 concentrations during this field campaign are shown in Fig.~~7a~~8a. The average HONO concentration during nighttime is higher than that during daytime due to the quick photolysis of HONO upon solar irradiation. The NH_3 concentration begins to increase in the morning (near 8~~ o'clock~~:00 LT) the reaches ~~the~~a plateau in the afternoon (8.5 to 15.5 ppb in average), and the SO_2 concentrations shows a similar diurnal variation to that of NH_3. This type of diurnal variation of SO_2 was also found by Xu et al. (2014), however, the cause of ~~this~~the common diurnal pattern ~~of~~between NH_3 and SO_2 during this field campaign requires further investigation. The NO_2 concentration increases quickly in the afternoon and decreases in the evening.

As shown in Fig.~~7b~~8b, the increase of NH_3 from morning to the afternoon was accompanied with the increase of mass fractions of nitrate and sulfate in $PM_{2.5}$ (The mass fractions of different aerosol chemical compositions were obtained by using the measured dry state PNSD to calculate volume concentration of $PM_{2.5}$, assuming that the density of aerosols in dry state is 1.5 g~~/cm^{3}~~ cm^{-3} (Yin et al., 2015). The results shown in Fig.~~7b~~8b indicate that the molecular concentration increase in nitrate ~~in~~from the morning ~~and~~to the afternoon is much faster than that of sulfate, ~~since the molar mass of sulfate is much higher than that of nitrate,~~ again supporting the ~~theory of~~fact that the NH_3-promoted NO_2 hydrolysis, which only produces HONO and nitrate directly~~. It is noteworthy that, in the morning,~~, was the main contributor to the observed explosive HONO formation. The evident morning increase of ~~the contribution of~~ inorganic aerosol ~~components (sulfate, nitrate, ammonium) to ambient aerosol mass~~component fractions resulted in prominent increases of aerosol hygroscopicity ~~(~~, displaying an average ~~hygroscopicity parameter κ~~κ anomaly of +0.04 during ~~this field campaign is 0.14 (Kuang et al., 2017) as shown in~~ noontime (Fig.~~7c.~~8c). From the morning to the afternoon, the ambient RH decreases quickly, however, the increase of aerosol hygroscopicity ~~will~~can retard the decrease of aerosol liquid water content and surface area density of ambient aerosols. ~~This~~This might acts as a positive feedback, further ~~enhances~~enhancing the hydrolysis of NO_2 as well as the nitrate and sulfate formation ~~as opposed to conditions with constant aerosol hygroscopicity~~.

5. Summary and atmospheric implications

Explosive HONO growth (observed maximum ~~dHONO/~~d[HONO]/dt=16.1 ppb~~/~~ h^{-1}) was observed for the first time on the NCP during fog and haze episodes with high RH conditions, only occurring with evident increases in NH_3, indicating that NH_3 is the key factor promoting the hydrolysis of NO_2, resulting in rapid HONO and nitrate formation. NH_3 ~~concentration~~concentrations during the observation period exhibit a distinct diurnal variation with an increase in the morning and a peak in the afternoon (8.5 to 15.5 ppb in average). The increase of NH_3 promotes the hydrolysis of NO_2, giving significant rise to HONO and nitrate concentrations. Produced HONO released OH radicals upon photolysis, which further oxidized SO_2 to sulfate through gas phase and heterogeneous reactions. Therefore, the significant ~~diurnal variations~~growth of NH_3 ~~has~~in the morning determined the ~~diurnal variations of~~increase in nitrate, sulfate and ammonium as well as that of aerosol hygroscopicity, which as a positive feedback retards the decrease in atmospheric liquid water content and further enhances the hydrolysis of NO_2 as well as the nitrate and sulfate formation.

Results in this paper reveals that the NH_3-promoted NO_2 hydrolysis is a significant source of HONO, which provides direct insight into the missing daytime source of HONO on the NCP. Results in this paper also shed light on the recent controversy of how SO_2, pH and NH_3 are involved in heterogeneous HONO production. It was clarified that ~~SO_2 does not directly take part~~ in the HONO production, ~~but is~~SO_2 took a minor part during fog events and an insignificant part during haze events, the observed growth in sulfate was dominantly the byproduct of the HONO photolysis, confirming again the importance HONO as an OH source and its crucial role in atmospheric chemistry.

These results have demonstrated the critical role and contribution of NH_3 in the formation of photochemical and aerosol pollution on the North China Plain. Effective control measures are urgently called for to reduce NH_3 emissions, which would simultaneously benefit the photochemical and aerosol pollution abatement through the reduction of HONO production.

Acknowledgments, Samples, and Data

This work is supported by the National Key R&D Program of China (2016YFC0202300), the National research program for key issues in air pollution control (DQGG0103) and the National Natural Science Foundation of China (41505107 and 41590872). We thank Wei Peng from Beijing Met High-Tech Co., Ltd. for his help with the maintenance of the IGAC instrument.

Author contributions. WX designed the experiment and YK led the research. YK, JT, GZ, YB, YY, CS and LL were responsible for the aerosol measurements in the experiment, WY helped with the IGAC measurements. WX made the trace gas measurements with the help of ZG, WL and XX. WX and YK analyzed the data and wrote the paper.

Competing interests. The authors declare that they have no conflictof interest

Data availability. The data used in this study are available from the corresponding author upon request (kuangye@jnu.edu.cn)

References

Cheng, Y., Zheng, G., Wei, C., Mu, Q., Zheng, B., Wang, Z., Gao, M., Zhang, Q., He, K., Carmichael, G., Pöschl, U., and Su, H.: Reactive nitrogen chemistry in aerosol water as a source of sulfate during haze events in China, Science Advances, 2, e1601530, 10.1126/sciadv.1601530, 2016.

Cui, L., Li, R., Zhang, Y., Meng, Y., Fu, H., and Chen, J.: An observational study of nitrous acid (HONO) in Shanghai, China: The aerosol impact on HONO formation during the haze episodes, The Science of the total environment, 630, 1057-1070, 10.1016/j.scitotenv.2018.02.063, 2018.

Ding, J., Zhao, P., Su, J., Dong, Q., and Du, X.: Aerosol pH and its influencing factors in Beijing, Atmos. Chem. Phys. Discuss., 2018, 1-34, 10.5194/acp-2018-270, 2018.

Guo, H., Weber, R. J., and Nenes, A.: High levels of ammonia do not raise fine particle pH sufficiently to yield nitrogen oxide-dominated sulfate production, Scientific reports, 7, 12109, 10.1038/s41598-017-11704-0, 2017.

Huang, R.-J., Yang, L., Cao, J., Wang, Q., Tie, X., Ho, K.-F., Shen, Z., Zhang, R., Li, G., Zhu, C., Zhang, N., Dai, W., Zhou, J., Liu, S., Chen, Y., Chen, J., and O'Dowd, C. D.: Concentration and sources of atmospheric nitrous acid (HONO) at an urban site in Western China, Science of The Total Environment, 593-594, 165-172, ~~https://doi.org/10.1016/j.scitotenv.2017.02.166,~~https://doi.org/10.1016/j.scitotenv.2017.02.166, 2017.

Kleffmann, J., Gavriloaiei, T., Hofzumahaus, A., Holland, F., Koppmann, R., Rupp, L., Schlosser, E., Siese, M., and Wahner, A.: Daytime formation of nitrous acid: A major source of OH radicals in a forest, Geophysical Research Letters, 32, doi:10.1029/2005GL022524, 2005.

Kuang, Y., Zhao, C. S., Tao, J. C., and Ma, N.: Diurnal variations of aerosol optical properties in the North China Plain and their influences on the estimates of direct aerosol radiative forcing, Atmos. Chem. Phys. Discuss., 15, 339-369, 10.5194/acpd-15-339-2015, 2015.

Kuang, Y., Zhao, C., Tao, J., Bian, Y., Ma, N., and Zhao, G.: A novel method for deriving the aerosol hygroscopicity parameter based only on measurements from a humidified nephelometer system, Atmos. Chem. Phys., 17, 6651-6662, 10.5194/acp-17-6651-2017, 2017.

Kuang, Y., Zhao, C. S., Zhao, G., Tao, J. C., Xu, W., Ma, N., and Bian, Y. X.: A novel method for calculating ambient aerosol liquid water content based on measurements of a humidified nephelometer system, Atmospheric Measurement Techniques, 11, 2967-2982, 10.5194/amt-11-2967-2018, 2018.

Li, L., Duan, Z., Li, H., Zhu, C., Henkelman, G., Francisco, J. S., and Zeng, X. C.: Formation of HONO from the NH3-promoted hydrolysis of NO2-dimers in the atmosphere, Proceedings of the National Academy of Sciences, 10.1073/pnas.1807719115, 2018a.

Li, L., Hoffmann, M. R., and Colussi, A. J.: Role of Nitrogen Dioxide in the Production of Sulfate during Chinese Haze-Aerosol Episodes, Environmental ~~science & technology~~Science & Technology, 52, 2686-2693, 10.1021/acs.est.7b05222, 2018b.

Li, X., Brauers, T., Häseler, R., Bohn, B., Fuchs, H., Hofzumahaus, A., Holland, F., Lou, S., Lu, K. D., Rohrer, F., Hu, M., Zeng, L. M., Zhang, Y. H., Garland, R. M., Su, H., Nowak, A., Wiedensohler, A., Takegawa, N., Shao, M., and Wahner, A.: Exploring the atmospheric chemistry of nitrous acid (HONO) at a rural site in Southern China, Atmospheric Chemistry and Physics, 12, 1497-1513, 10.5194/acp-12-1497-2012, 2012.

Liu, M., Song, Y., Zhou, T., Xu, Z., Yan, C., Zheng, M., Wu, Z., Hu, M., Wu, Y., and Zhu, T.: Fine particle pH during severe haze episodes in northern China, Geophysical Research Letters, 44, 5213-5221, doi:10.1002/2017GL073210, 2017a.

Liu, Y., Wu, Z., Wang, Y., Xiao, Y., Gu, F., Zheng, J., Tan, T., Shang, D., Wu, Y., Zeng, L., Hu, M., Bateman, A. P., and Martin, S. T.: Submicrometer Particles Are in the Liquid State during Heavy Haze Episodes in the Urban Atmosphere of Beijing, China, Environmental Science & Technology Letters, 4, 427-432, 10.1021/acs.estlett.7b00352, 2017b.

Liu, Z., Wang, Y., Costabile, F., Amoroso, A., Zhao, C., Huey, L. G., Stickel, R., Liao, J., and Zhu, T.: Evidence of Aerosols as a Media for Rapid Daytime HONO Production over China, Environmental ~~science & technology~~Science & Technology, 48, 14386-14391, 10.1021/es504163z, 2014.

Lu, C., Niu, S., Tang, L., Lv, J., Zhao, L., and Zhu, B.: Chemical composition of fog water in Nanjing area of China and its related fog microphysics, Atmospheric Research, 97, 47-69, http://dx.doi.org/10.1016/j.atmosres.2010.03.007, 2010.

Lu, K., Guo, S., Tan, Z., Wang, H., Shang, D., Liu, Y., Li, X., Wu, Z., Hu, M., and Zhang, Y.: Exploring atmospheric free-radical chemistry in China: the self-cleansing capacity and the formation of secondary air pollution, National Science Review, nwy073-nwy073, 10.1093/nsr/nwy073, 2018.

Meng, Z., Xu, X., Lin, W., Ge, B., Xie, Y., Song, B., Jia, S., Zhang, R., Peng, W., Wang, Y., Cheng, H., Yang, W., and Zhao, H.: Role of ambient ammonia in particulate ammonium formation at a rural site in the North China Plain, Atmos. Chem. Phys., 18, 167-184, 10.5194/acp-18-167-2018, 2018.

Michoud, V., Colomb, A., Borbon, A., Miet, K., Beekmann, M., Camredon, M., Aumont, B., Perrier, S., Zapf, P., Siour, G., Ait-Helal, W., Afif, C., Kukui, A., Furger, M., Dupont, J. C., Haeffelin, M., and Doussin, J. F.: Study of the unknown HONO daytime source at a European suburban site during the MEGAPOLI summer and winter field campaigns, Atmos. Chem. Phys., 14, 2805-2822, 10.5194/acp-14-2805-2014, 2014.

Nie, W., Ding, A. J., Xie, Y. N., Xu, Z., Mao, H., Kerminen, V. M., Zheng, L. F., Qi, X. M., Huang, X., Yang, X. Q., Sun, J. N., Herrmann, E., Petäjä, T., Kulmala, M., and Fu, C. B.: Influence of biomass burning plumes on HONO chemistry in eastern China, ~~Atmospheric Chemistry and Physics,~~Atmos. Chem. Phys., 15, 1147-1159, 10.5194/acp-15-1147-2015, 2015.

Petters, M. D., and Kreidenweis, S. M.: A single parameter representation of hygroscopic growth and cloud condensation nucleus activity, Atmospheric Chemistry and Physics, 7, 1961-1971, 2007.

Ran, L., Zhao, C. S., Xu, W. Y., Lu, X. Q., Han, M., Lin, W. L., Yan, P., Xu, X. B., Deng, Z. Z., Ma, N., Liu, P. F., Yu, J., Liang, W. D., and Chen, L. L.: VOC reactivity and its effect on ozone production during the HaChi summer campaign, Atmos. Chem. Phys., 11, 4657-4667, 10.5194/acp-11-4657-2011, 2011.

Safai, P. D., Kewat, S., Pandithurai, G., Praveen, P. S., Ali, K., Tiwari, S., Rao, P. S. P., Budhawant, K. B., Saha, S. K., and Devara, P. C. S.: Aerosol characteristics during winter fog at Agra, North India, J. Atmos. Chem., 61, 101-118, 10.1007/s10874-009-9127-4, 2008.

Shen, C., Zhao, C., Ma, N., Tao, J., Zhao, G., Yu, Y., and Kuang, Y.: Method to Estimate Water Vapor Supersaturation in the Ambient Activation Process Using Aerosol and Droplet Measurement Data, Journal of Geophysical Research: Atmospheres, 123, 10606-10619, doi:10.1029/2018JD028315, 2018.

Song, S., Gao, M., Xu, W., Shao, J., Shi, G., Wang, S., Wang, Y., Sun, Y., and McElroy, M. B.: Fine-particle pH for Beijing winter haze as inferred from different thermodynamic equilibrium models, Atmos. Chem. Phys., 18, 7423-7438, 10.5194/acp-18-7423-2018, 2018.

Stutz, J., Alicke, B., and Neftel, A.: Nitrous acid formation in the urban atmosphere: Gradient measurements of NO2 and HONO over grass in Milan, Italy, Journal of Geophysical Research: Atmospheres, 107, LOP 5-1-LOP 5-15, doi:10.1029/2001JD000390, 2002.

Su, H., Cheng, Y., Oswald, R., Behrendt, T., Trebs, I., Meixner, F. X., Andreae, M. O., Cheng, P., Zhang, Y., and Pöschl, U.: Soil Nitrite as a Source of Atmospheric HONO and OH Radicals, Science, 333, 1616-1618, 10.1126/science.1207687, 2011.

Teng, X., Hu, Q., Zhang, L., Qi, J., Shi, J., Xie, H., Gao, H., and Yao, X.: Identification of Major Sources of Atmospheric NH3 in an Urban Environment in Northern China During Wintertime, Environmental Science & Technology, 51, 6839-6848, 10.1021/acs.est.7b00328, 2017.

Vogel, B., Vogel, H., Kleffmann, J., and Kurtenbach, R.: Measured and simulated vertical profiles of nitrous acid—Part II. Model simulations and indications for a photolytic source, Atmospheric Environment, 37, 2957-2966, https://doi.org/10.1016/S1352-2310(03)00243-7, 2003.

Wang, G., Zhang, R., Gomez, M. E., Yang, L., Levy Zamora, M., Hu, M., Lin, Y., Peng, J., Guo, S., Meng, J., Li, J., Cheng, C., Hu, T., Ren, Y., Wang, Y., Gao, J., Cao, J., An, Z., Zhou, W., Li, G., Wang, J., Tian, P., Marrero-Ortiz, W., Secrest, J., Du, Z., Zheng, J., Shang, D., Zeng, L., Shao, M., Wang, W., Huang, Y., Wang, Y., Zhu, Y., Li, Y., Hu, J., Pan, B., Cai, L., Cheng, Y., Ji, Y., Zhang, F., Rosenfeld, D., Liss, P. S., Duce, R. A., Kolb, C. E., and Molina, M. J.: Persistent sulfate formation from London Fog to Chinese haze, Proceedings of the National Academy of Sciences, ~~113, 13630, 2016a~~10.1073/pnas.1616540113, 2016.

~~Wang, G., Zhang, R., Gomez, M. E., Yang, L., Levy Zamora, M., Hu, M., Lin, Y., Peng, J., Guo, S., Meng, J., Li, J., Cheng, C., Hu, T., Ren, Y., Wang, Y., Gao, J., Cao, J., An, Z., Zhou, W., Li, G., Wang, J., Tian, P., Marrero-Ortiz, W., Secrest, J., Du, Z., Zheng, J., Shang, D., Zeng, L., Shao, M., Wang, W., Huang, Y., Wang, Y., Zhu, Y., Li, Y., Hu, J., Pan, B., Cai, L., Cheng, Y., Ji, Y., Zhang, F., Rosenfeld, D., Liss, P. S., Duce, R. A., Kolb, C. E., and Molina, M. J.: Persistent sulfate formation from London Fog to Chinese haze, Proc Natl Acad Sci U S A, 10.1073/pnas.1616540113, 2016b.~~

Whalley, L. K., Stone, D., George, I. J., Mertes, S., van Pinxteren, D., Tilgner, A., Herrmann, H., Evans, M. J., and Heard, D. E.: The influence of clouds on radical concentrations: observations and modelling studies of HO_x during the Hill Cap Cloud Thuringia (HCCT) campaign in 2010, Atmos. Chem. Phys., 15, 3289-3301, 10.5194/acp-15-3289-2015, 2015.

Wu, Z., Wang, Y., Tan, T., Zhu, Y., Li, M., Shang, D., Wang, H., Lu, K., Guo, S., Zeng, L., and Zhang, Y.: Aerosol Liquid Water Driven by Anthropogenic Inorganic Salts: Implying Its Key Role in Haze Formation over the North China Plain, Environmental Science & Technology Letters, 10.1021/acs.estlett.8b00021, 2018.

Xing, J., Ding, D., Wang, S., Zhao, B., Jang, C., Wu, W., Zhang, F., Zhu, Y., and Hao, J.: Quantification of the enhanced effectiveness of NOx control from simultaneous reductions of VOC and NH3 for reducing air pollution in the Beijing–Tianjin–Hebei region, China, Atmos. Chem. Phys., 18, 7799-7814, 10.5194/acp-18-7799-2018, 2018.

Xu, W. Y., Zhao, C. S., Ran, L., Lin, W. L., Yan, P., and Xu, X. B.: SO2 noontime-peak phenomenon in the North China Plain, Atmospheric Chemistry and Physics, 14, 7757-7768, 10.5194/acp-14-7757-2014, 2014.

Xue, L. K., Wang, T., Gao, J., Ding, A. J., Zhou, X. H., Blake, D. R., Wang, X. F., Saunders, S. M., Fan, S. J., Zuo, H. C., Zhang, Q. Z., and Wang, W. X.: Ground-level ozone in four Chinese cities: precursors, regional transport and heterogeneous processes, Atmos. Chem. Phys., 14, 13175-13188, 10.5194/acp-14-13175-2014, 2014.

Yabushita, A., Enami, S., Sakamoto, Y., Kawasaki, M., Hoffmann, M. R., and Colussi, A. J.: Anion-Catalyzed Dissolution of NO2 on Aqueous Microdroplets, The Journal of Physical Chemistry A, 113, 4844-4848, 10.1021/jp900685f, 2009.

Ye, C., Liu, P., Ma, Z., Xue, C., Zhang, C., Zhang, Y., Liu, J., Liu, C., Sun, X., and Mu, Y.: High H2O2 Concentrations Observed during Haze Periods during the Winter in Beijing: Importance of H2O2 Oxidation in Sulfate Formation, Environmental Science & Technology Letters, 10.1021/acs.estlett.8b00579, 2018.

Yin, Z., Ye, X., Jiang, S., Tao, Y., Shi, Y., Yang, X., and Chen, J.: Size-resolved effective density of urban aerosols in Shanghai, Atmospheric Environment, 100, 133-140, http://dx.doi.org/10.1016/j.atmosenv.2014.10.055, 2015.

Young, L.-H., Li, C.-H., Lin, M.-Y., Hwang, B.-F., Hsu, H.-T., Chen, Y.-C., Jung, C.-R., Chen, K.-C., Cheng, D.-H., Wang, V.-S., Chiang, H.-C., and Tsai, P.-J.: Field performance of a semi-continuous monitor for ambient PM2.5 water-soluble inorganic ions and gases at a suburban site, Atmospheric Environment, 144, 376-388, ~~https://doi.org/10.1016/j.atmosenv.2016.08.062,~~https://doi.org/10.1016/j.atmosenv.2016.08.062, 2016.

Zheng, G. J., Duan, F. K., Su, H., Ma, Y. L., Cheng, Y., Zheng, B., Zhang, Q., Huang, T., Kimoto, T., Chang, D., Pöschl, U., Cheng, Y. F., and He, K. B.: Exploring the severe winter haze in Beijing: the impact of synoptic weather, regional transport and heterogeneous reactions, Atmos. Chem. Phys., 15, 2969-2983, 10.5194/acp-15-2969-2015, 2015.

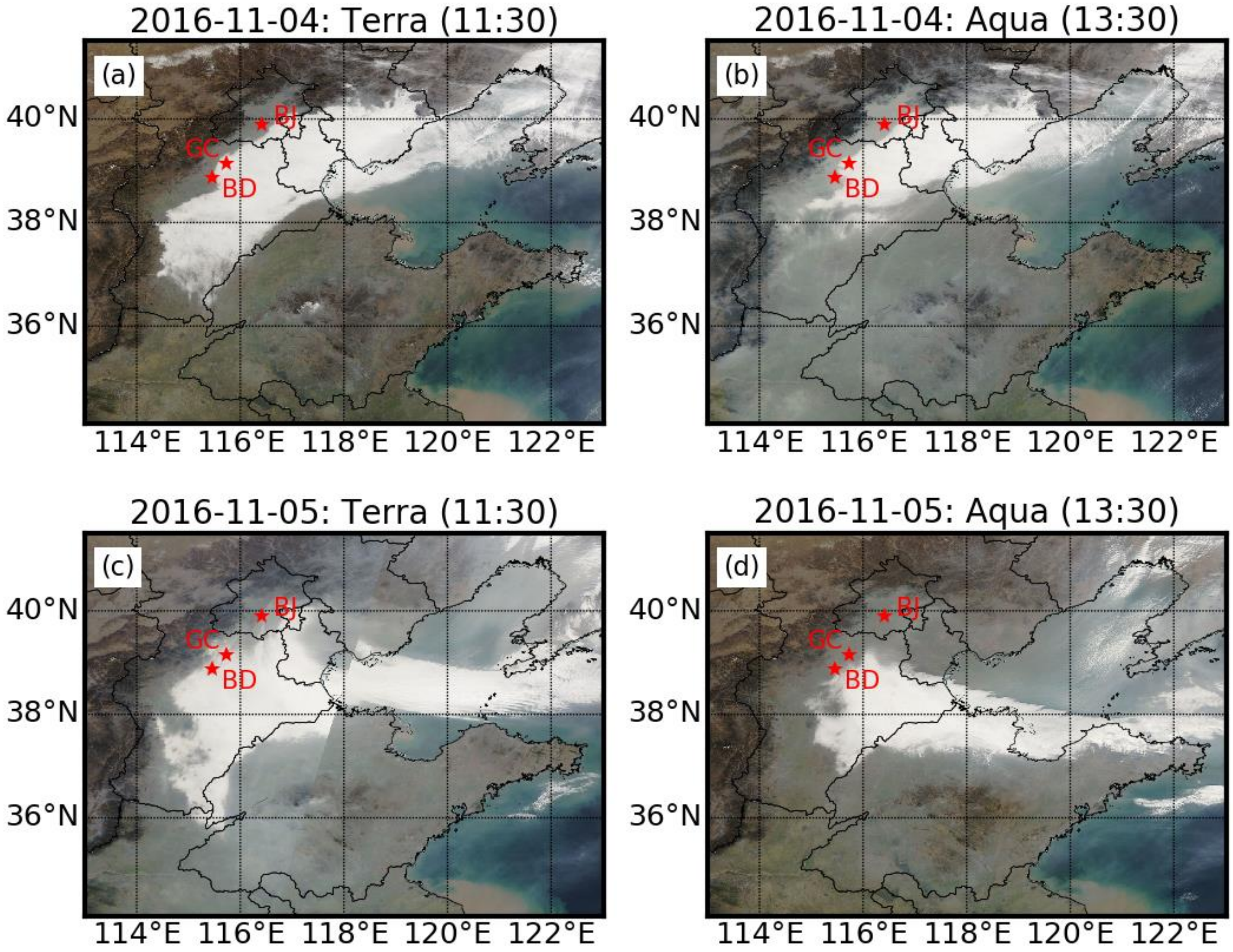

Figure 1. MODIS Terra (a,c) and Aqua (b,d) satellite images in ~~2016-11-04~~04th Nov. (a,b) and 5th Nov. 2016~~-11-05~~ (c,d), star markers are locations of Gucheng (GC: the observation site), Baoding (BD) and Beijing (BJ).

807

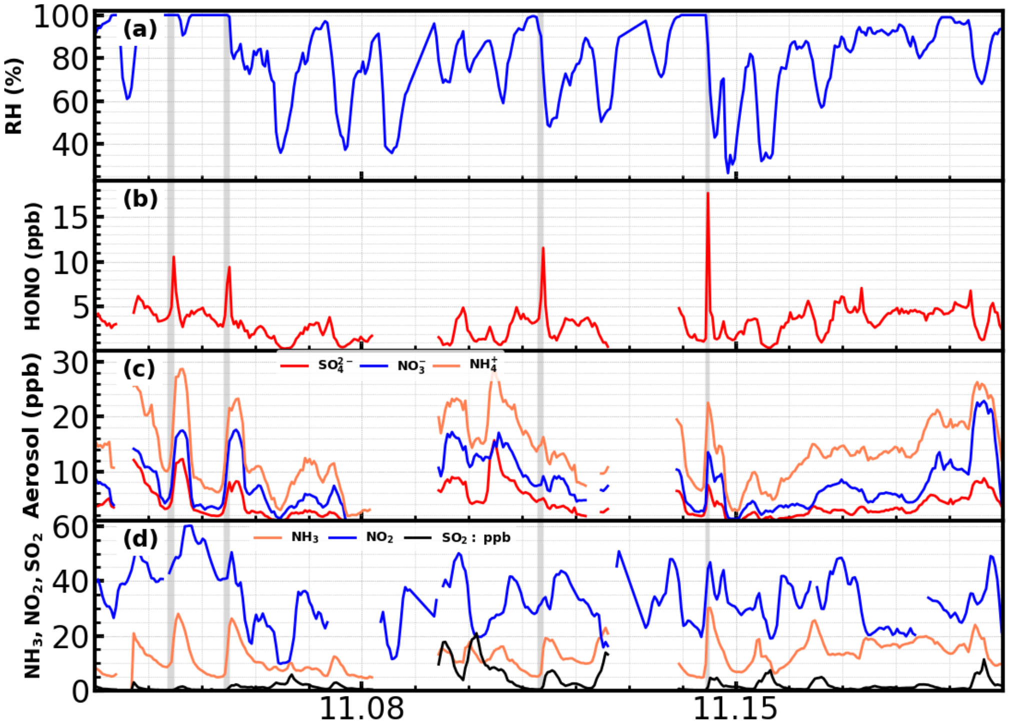
RH (%)
100
80
60
40
(a)
HONO (ppb)
15
10
5
(b)
Aerosol (ppb)
30
20
10
(c)
SO_4^{2-}
NO_3^-
NH_4^+
NH_3, NO_2, SO_2
60
40
20
0
(d)
NH_3
NO_2
SO_2 : ppb
11.08
11.15

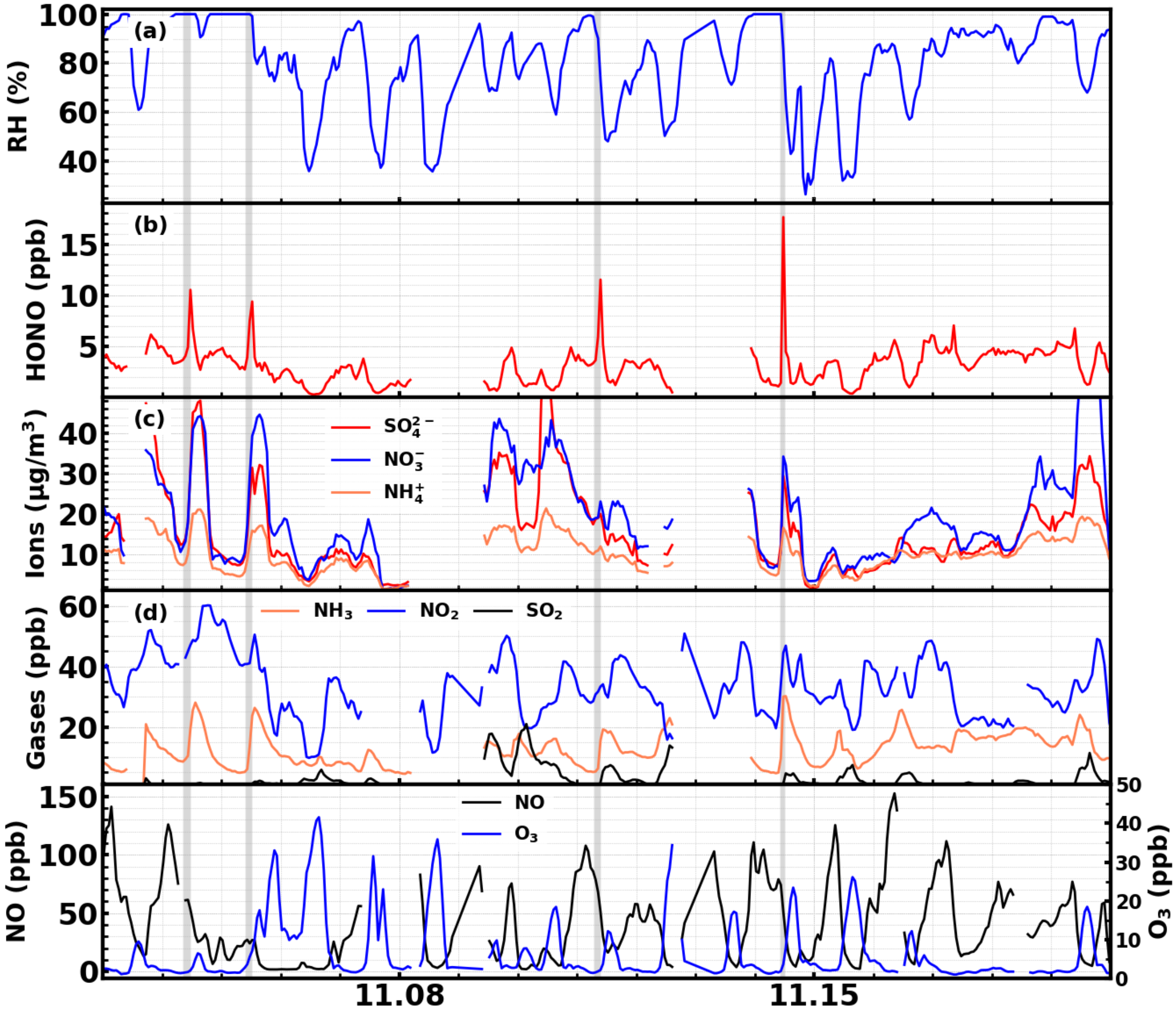

Figure 2. Time series of ambient **a)** RH; **b)** HONO; **c)** sulfate, nitrate, ammonium; **d)** NH_3, NO_3 and SO_2 during the observation period.

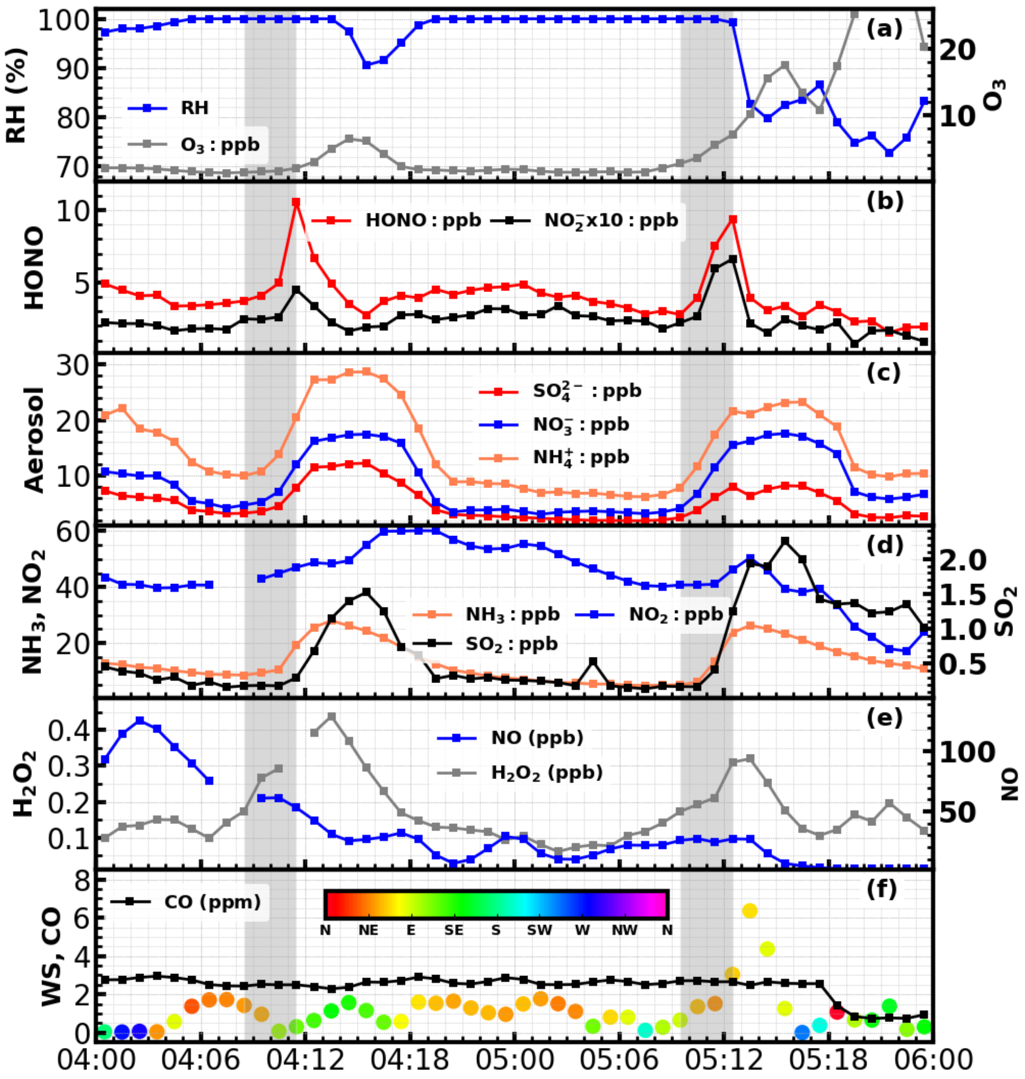
(a)
RH (%)
100
90
80
70
RH
O_3 : ppb
O_3
20
10
(b)
HONO
10
5
HONO : ppb
NO_2^-x10 : ppb
(c)
Aerosol
30
20
10
SO_4^{2-} : ppb
NO_3^- : ppb
NH_4^+ : ppb
(d)
NH_3, NO_2
60
40
20
NH_3 : ppb
NO_2 : ppb
SO_2 : ppb
SO_2
2.0
1.5
1.0
0.5
(e)
H_2O_2
0.4
0.3
0.2
0.1
NO (ppb)
H_2O_2 (ppb)
NO
100
50
(f)
WS, CO
8
6
4
2
0
CO (ppm)
N
NE
E
SE
S
SW
W
NW
N
04:00
04:06
04:12
04:18
05:00
05:06
05:12
05:18
06:00

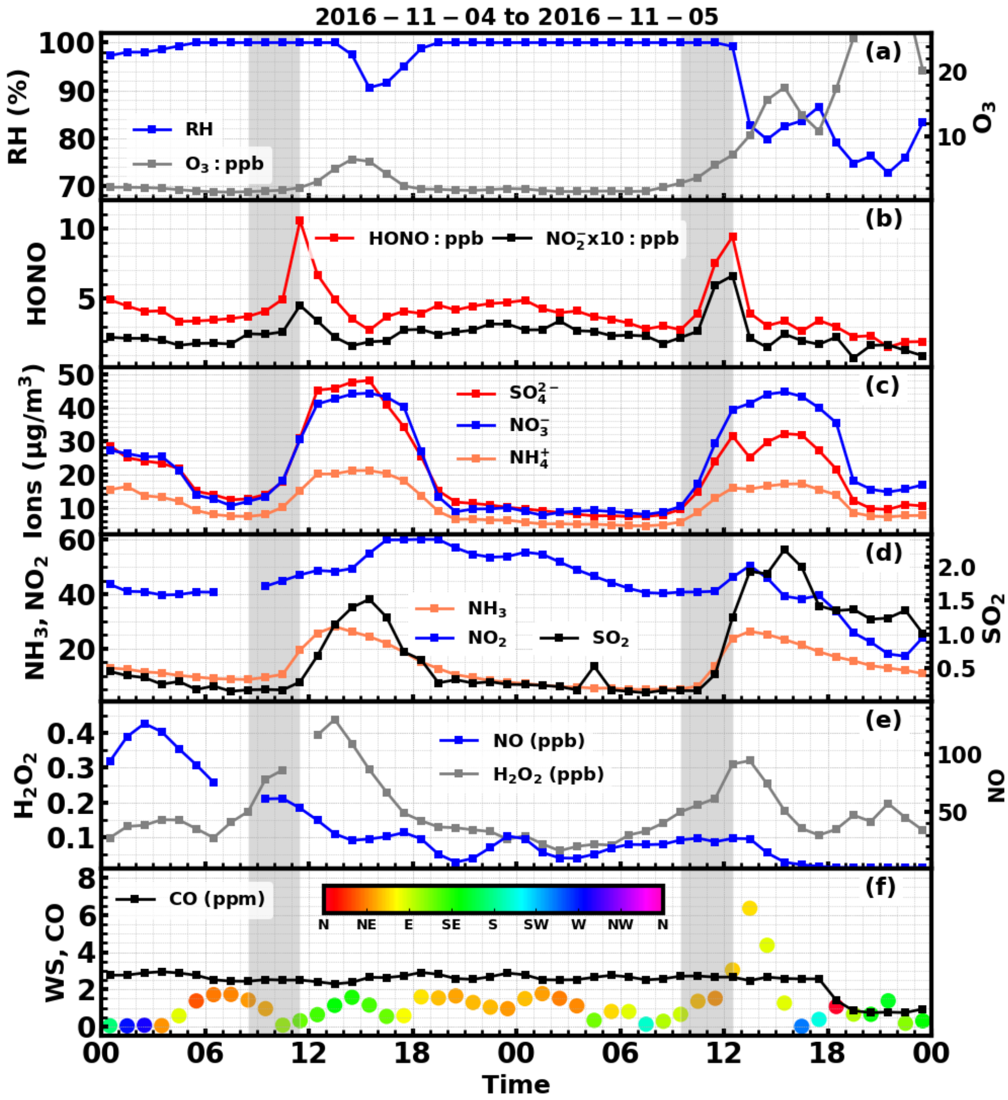

Figure 3. Time series of ambient **a)** RH,O_3, **b)**HONO, NO_2^-, **c)** SO_4^{2-}, NO_3^-, NH_4^+, **d)** NH_3, NO_2, SO_2, **e)** NO, H_2O_2, **f)** CO, wind speed and wind direction (colors of scatter points) from ~~11-04~~4th to ~~11-05~~5th Nov. 2016. Gray shaded areas represent periods of rapid increase of HONO.

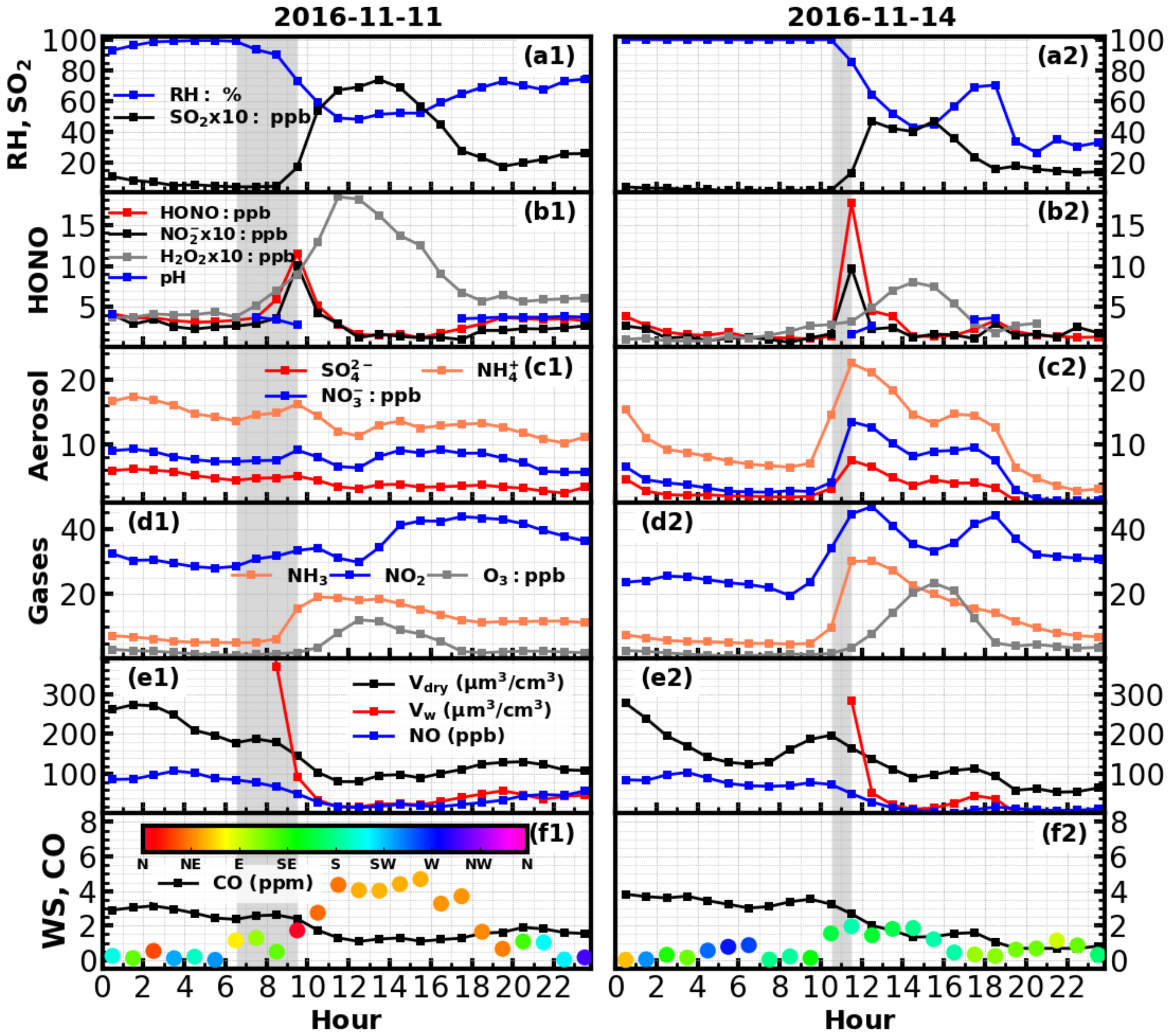
2016-11-11
2016-11-14
RH, SO$_2$
(a1)
(a2)
RH : %
SO$_2$x10 : ppb
HONO
(b1)
(b2)
HONO : ppb
NO$_2^-$x10 : ppb
H$_2$O$_2$x10 : ppb
pH
Aerosol
(c1)
(c2)
SO$_4^{2-}$
NH$_4^+$
NO$_3^-$: ppb
Gases
(d1)
(d2)
NH$_3$
NO$_2$
O$_3$: ppb
(e1)
(e2)
V$_{dry}$ (μm^3/cm^3)
V$_w$ (μm^3/cm^3)
NO (ppb)
WS, CO
(f1)
(f2)
N NE E SE S SW W NW N
CO (ppm)
Hour
Hour

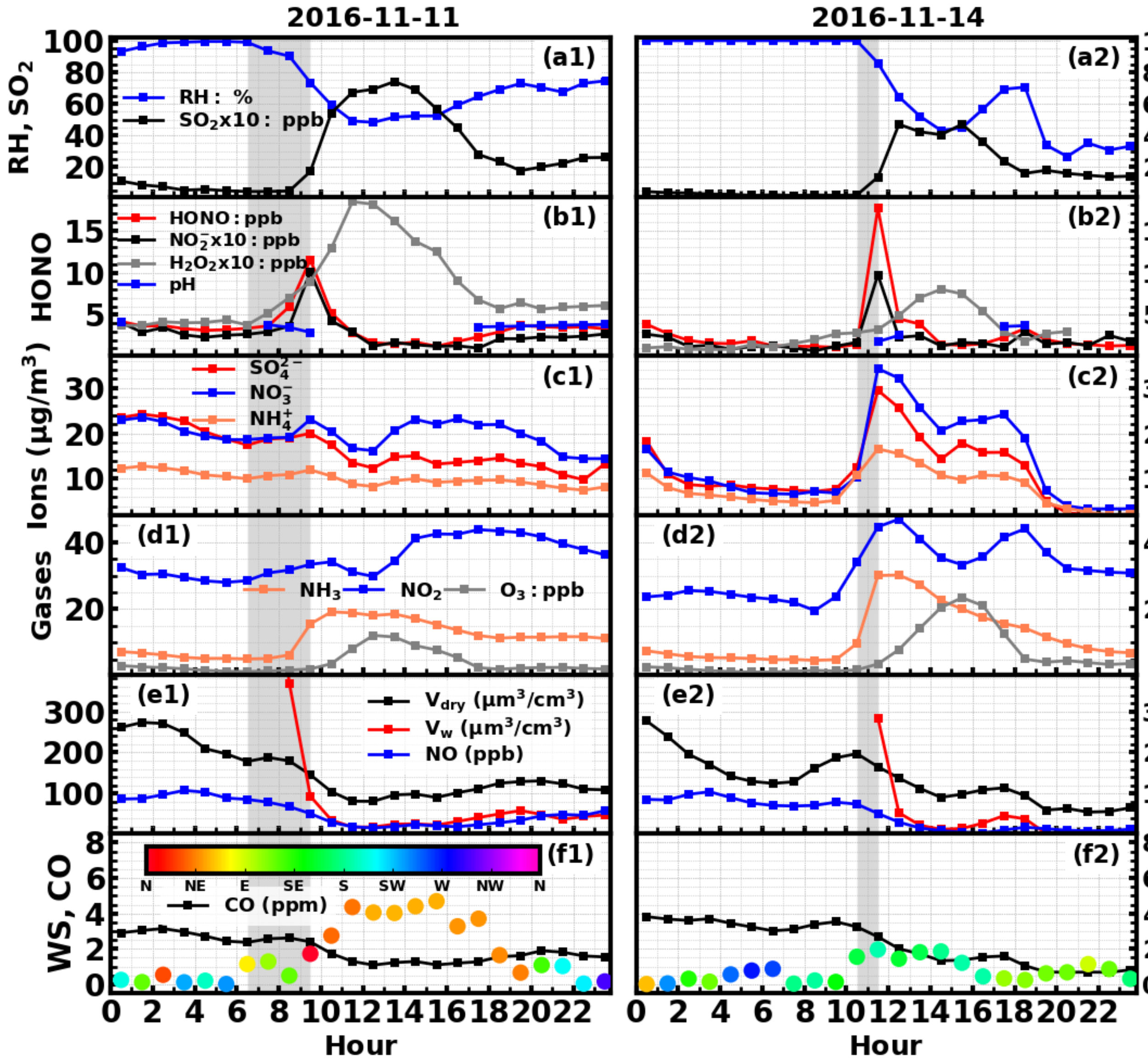

Figure 4. Time series of ambient **a)** RH, SO_2, **b)** HONO, NO_2^-, H_2O_2, aerosol pH, **c)** SO_4^{2-}, NO_3^-, NH_4^+,**d)** NH_3, NO_2, O_3, **e)** NO, volume concentrations of $PM_{2.5}$ in dry state (V_{dry}), volume concentrations of liquid water (V_w), **f)** CO, wind speed and wind direction during **1)** 11th Nov. 2016 and **2)** 14th Nov. 2016. Gray shaded areas represents periods of rapid increase of HONO.

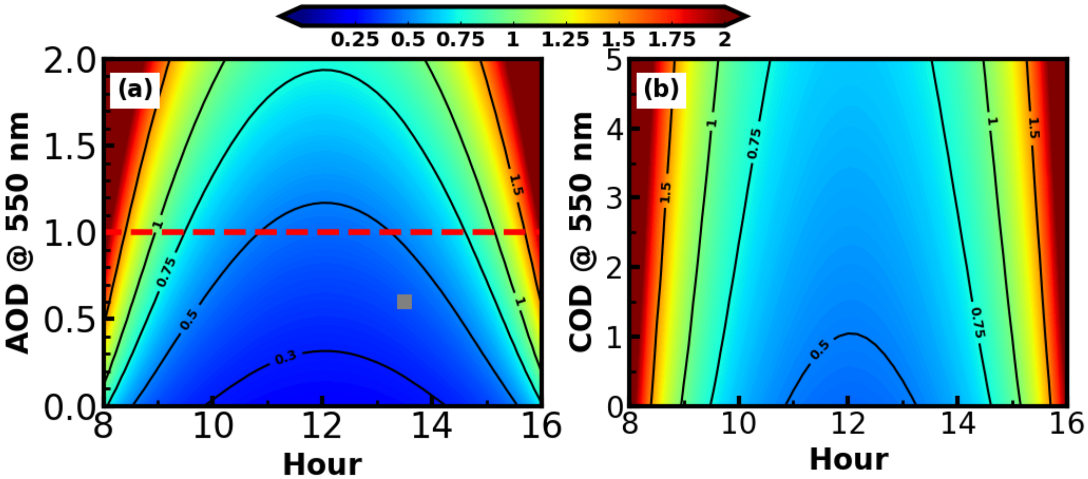

~~**Figure 5**. **(a)** Diurnal variations of lifetime of HONO under different aerosol optical depth (AOD) conditions. Gray solid marker represents the AOD position from MODIS Aqua in 2016-11-14 (about 13:30); **(b)** Diurnal variations of lifetime of HONO under different cloud optical depth (COD) conditions, with an AOD of 1.~~

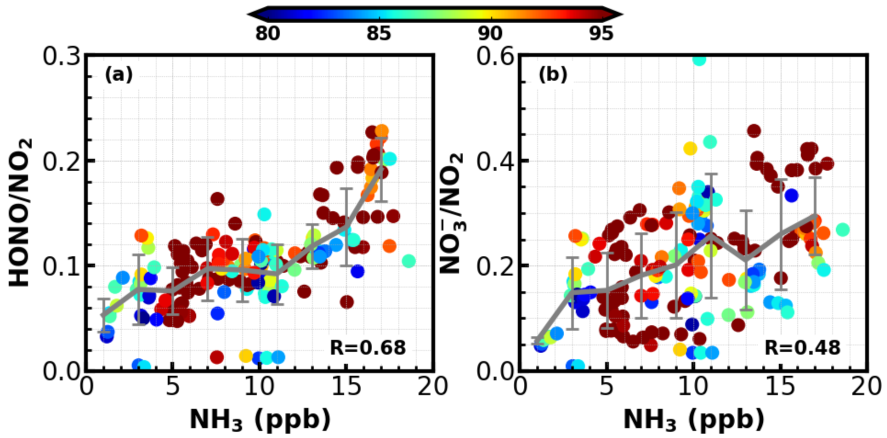

~~**Figure 6.**~~

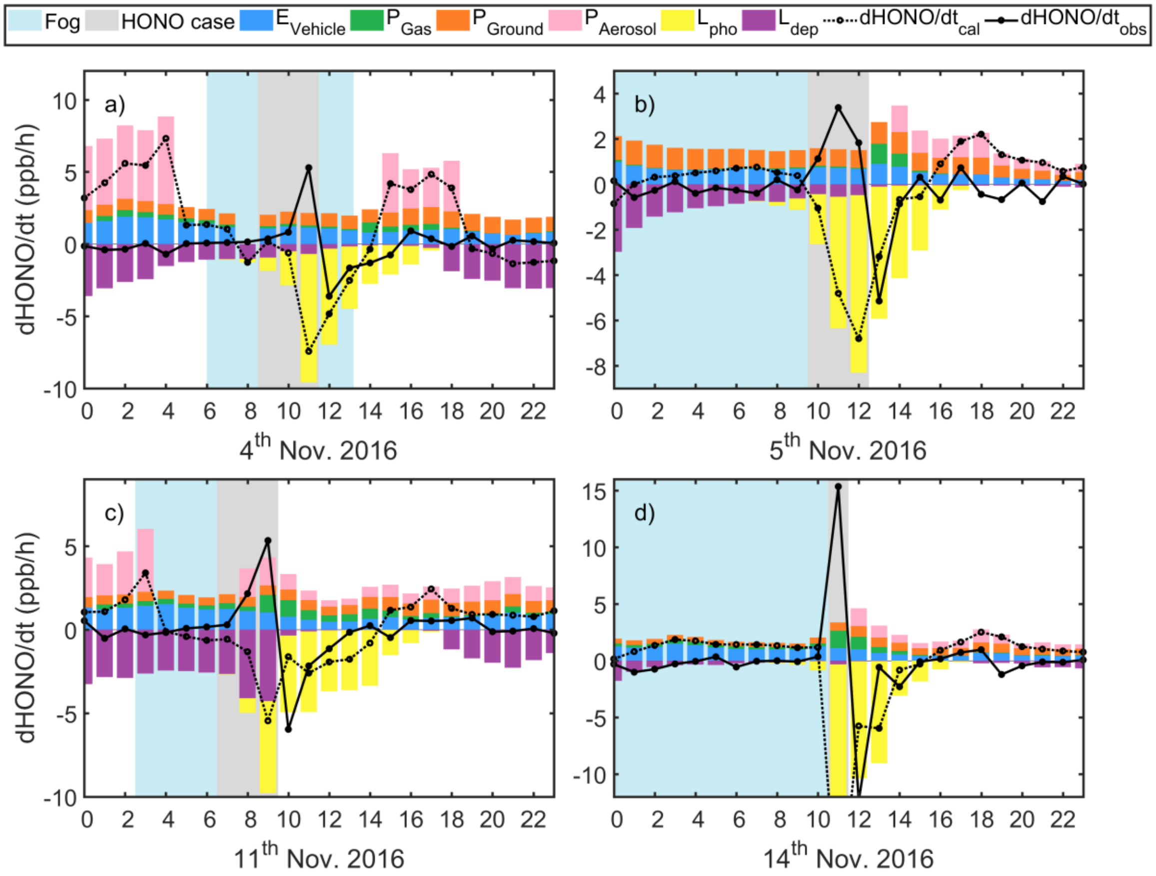

Figure 5. Estimated HONO emission from vehicles (blue), gas phase production (green), production on ground (orange) and aerosol surface (pink), loss through photolysis (yellow) and dry deposition (purple), as well as the calculated (dotted black) and actually observed (solid black) d[HONO]/dt on a) 4th, b) 5th, c) 11th and d) 14th Nov. 2016

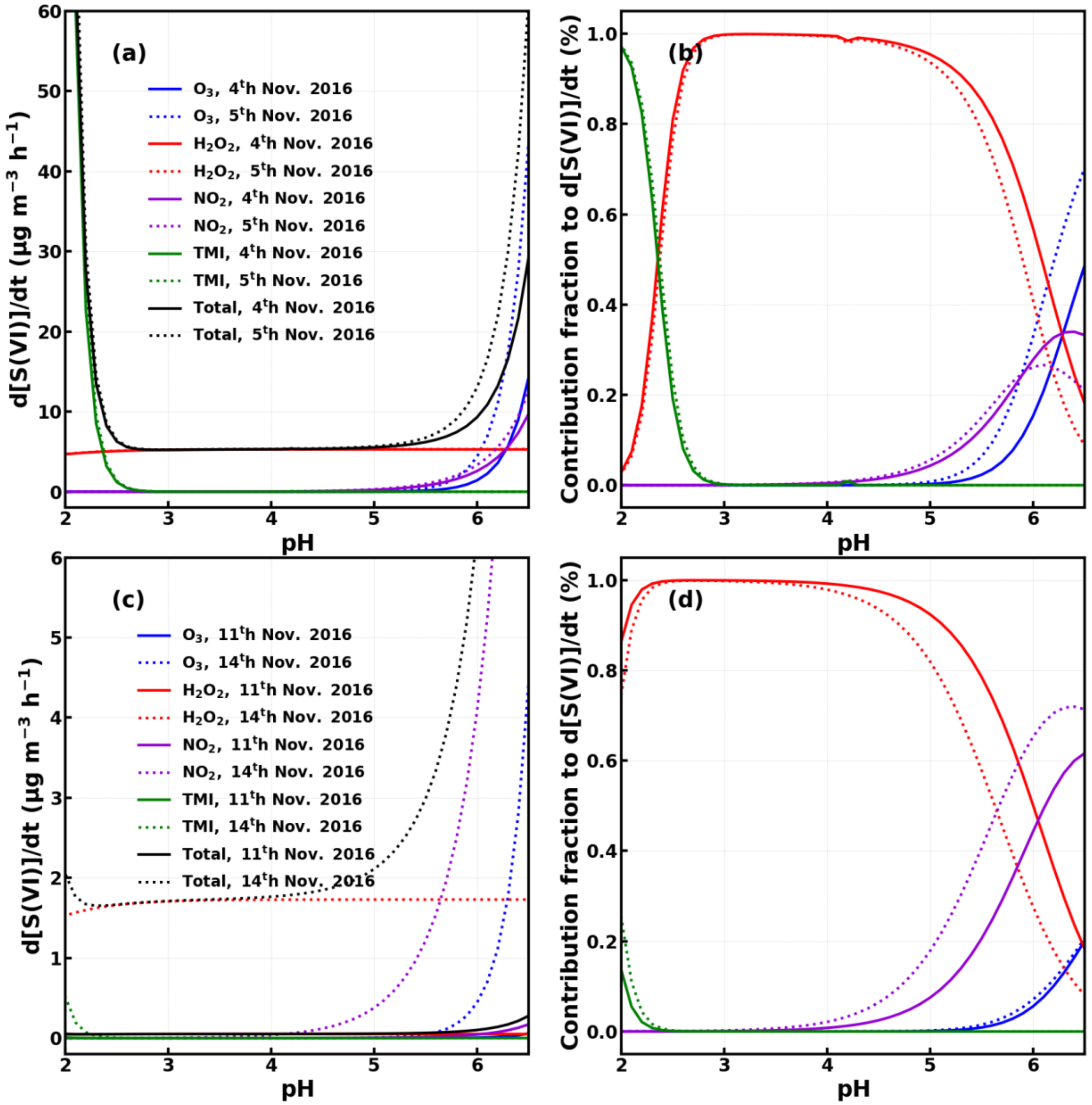

Figure 6. Calculated average sulfate production (a,c) and contribution fraction b,d) from SO_2 oxidation by H_2O_2, NO_2, O_3, TMI under different pH values using methods described in (Cheng et al., 2016) for the case episodes on 4th, 5th, 11th and 14th Nov. 2016.

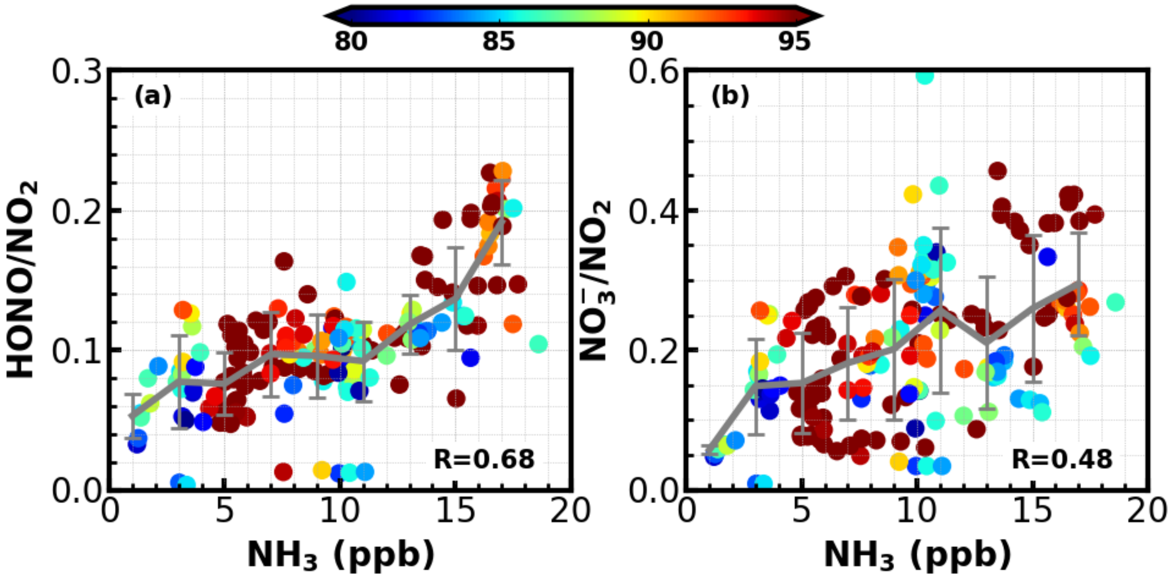

Figure 7. The relationship between NH_3 concentration and **a)** HONO/NO_2 ratio; **b)** nitrate/nitrogen dioxide ratio (NO_3^-/NO_2); Colors of scatter points represent ambient RHs and the color bar is shown on the top.

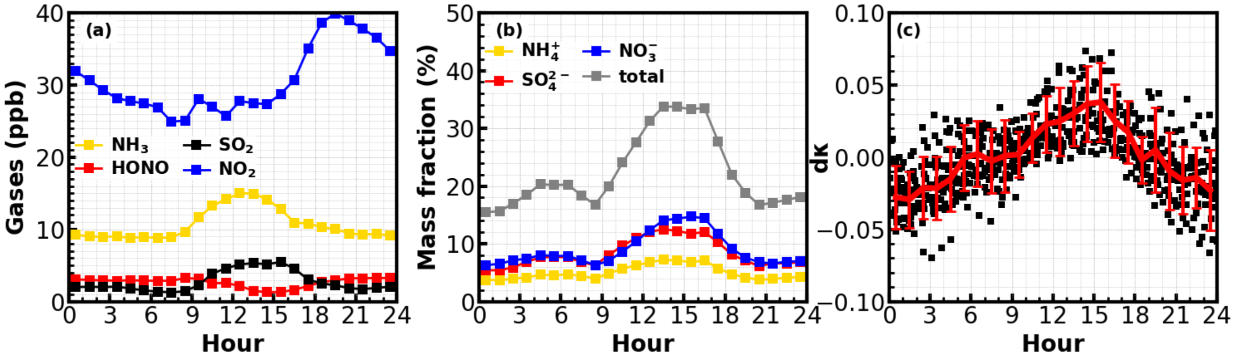

Figure ~~7~~8. **(a)** Average diurnal variations of Gases~~-~~; **(b)** Average diurnal variations mass fractions of nitrate, sulfate and ammonium; **(c)** Diurnal variations of aerosol hygroscopicity, dκ is the anomaly to the daily mean κ.